Graduate School Form 30
(Revised 08/14)

PURDUE UNIVERSITY
GRADUATE SCHOOL
Thesis/Dissertation Acceptance

This is to certify that the thesis/dissertation prepared

By Arika Kemp

Entitled
Peripheral Venous Retroperfusion: Implications for Critical Limb Ischemia and Salvage

For the degree of Master of Science in Biomedical Engineering

Is approved by the final examining committee:

Ghassan Kassab

Joseph Unthank

William Combs

To the best of my knowledge and as understood by the student in the Thesis/Dissertation Agreement, Publication Delay, and Certification/Disclaimer (Graduate School Form 32), this thesis/dissertation adheres to the provisions of Purdue University's "Policy on Integrity in Research" and the use of copyrighted material.

Ghassan Kassab

Approved by Major Professor(s): _____

_____

Approved by: Ken Yoshida 11/24/2014

Head of the Department Graduate Program Date

PERIPHERAL VENOUS RETROPERFUSION: IMPLICATIONS FOR CRITICAL LIMB ISCHEMIA AND SALVAGE

A Thesis

Submitted to the Faculty

of

Purdue University

by

Arika D. Kemp

In Partial Fulfillment of the

Requirements for the Degree

of

Master of Science in Biomedical Engineering

December 2014

Purdue University

Indianapolis, Indiana

In memory of my papaw. Your short time here left everlasting footprints in countless lives. May the cardiovascular disease and diabetes that took your life be the ambition behind all my life's work.

ACKNOWLEDGMENTS

I would like to thank my advisor, Dr. Ghassan Kassab, and committee members, Dr. Joseph Unthank and Bill Combs, for all their time, support, incredible advice, invaluable comments, and effort throughout the study. A special thanks to my mentors, Dr. Zachary Berwick and Dr. Mark Svendsen, whom made the study possible, taught me the skills and expertise required for the study, and continued to push and encourage me throughout my graduate studies. A thanks to Adam Essex and Leon Carter for their help in the surgery room and to Dr. Hyowon Choi for his computation advice on the study. A thanks to my boyfriend, Chad Harding, for his patience, support, and help with making figures for my thesis. A final thanks to the IUPUI BME Department for awarding me with the Research Assistantship and their genuine support and encouragement throughout my graduate studies.

TABLE OF CONTENTS

Page

LIST OF TABLES vii

LIST OF FIGURES viii

ABSTRACT x

1 INTRODUCTION 1

1.1 Background 1

1.1.1 Cardiovascular System 1

1.1.1.1 Anatomy and Physiology 2

1.1.1.2 Vasculature Components 3

1.1.1.3 Microcirculation 6

1.1.1.4 Hemodynamics 9

1.1.2 Disease 10

1.1.2.1 Development 10

1.1.2.2 Plaque Formation 11

1.1.2.3 Blockages 11

1.1.2.4 Atherosclerosis 11

1.1.3 Peripheral Arterial Disease 12

1.1.3.1 Risk Factors 12

1.1.3.2 Progression of PAD 13

1.1.3.3 Atherosclerotic Lesions 15

1.1.3.4 Treatment Options 15

1.1.4 Retroperfusion 17

1.1.4.1 History 18

1.1.4.2 Limitations 22

1.1.4.2.1 In-situ Retroperfusion 22

Page
1.1.4.2.2 Excised Retroperfusion 24
1.2 Objectives 25
1.2.1 Hypothesis 26
1.3 Methods 26
2 OBJECTIVES 28
2.1 Specific Aims 28
2.1.1 Specific Aim 1 28
2.1.2 Specific Aim 2 28
2.1.2.1 Specific Aim 2A 29
2.1.2.2 Specific Aim 2B 29
2.1.2.3 Specific Aim 2C 29
2.1.3 Specific Aim 3 29
2.1.3.1 Specific Aim 3A 30
2.1.3.2 Specific Aim 3B 30
2.1.3.3 Specific Aim 3C 30
2.1.4 Specific Aim 4 30
3 METHODS 32
3.1 Theoretical Basis 32
3.2 Ex-vivo Experiments 33
3.3 In-vivo Experiments 37
3.4 Theoretical Assessment 44
3.5 Statistical Analysis 45
4 RESULTS 47
4.1 Theoretical Basis 47
4.2 Ex-vivo Experiments 47
4.3 In-vivo Experiments 53
4.4 Theoretical Assessment 58
5 DISCUSSION 62

Page

5.1 Determine how the Catheter Resistance Relates to the Physiological System. 63

5.2 Determine the Resistance of the Venous Retro-Vasculature Most Suitable for Effective Retroperfusion. 65

5.2.1 Determine Whether Flow Reversals are Possible. 65

5.2.2 Determine if the Retroperfusion Hemodynamics is Location Dependent. 65

5.2.3 Determine What Location Seems Most Promising for Effective Retroperfusion. 68

5.3 Determine the Resistance of the Venous Retro-Vasculature and Characteristics of Retroperfusion In vivo. 70

5.3.1 Determine the Active Hemodynamics at the Retroperfusion Site. 71

5.3.2 Determine the Perfusion Territory of Venous Reversed Flow Compared to Arterial Forward Flow. 72

5.3.3 Determine the Effects of Retroperfusion on an Acute Hindlimb Ischemia Canine Model. 73

5.4 Determine the Ideal Catheter Resistance Given the Hemodynamic Data Retrieved in In-vivo Experiments. 74

6 CONCLUSIONS 76

6.1 Limitations and Future Work 76

REFERENCES 80

LIST OF TABLES

Table Page

4.1 Parameters of the Theoretical Circuit 48

4.2 Blood Gas Results of Inflow and Outflow Blood Samples 57

4.3 Ideal Catheter Resistance Given an Inlet Pressure, a Catheter Output Pressure Equal to In-vivo Data, and Inlet Flow Rates 59

LIST OF FIGURES

Figure		Page
1.1	Basic schematic of the cardiovascular system	3
1.2	Structure breakdown of blood vessels	4
1.3	Pressure dynamics of the vasculature	6
1.4	The driving forces acting on a capillary	8
1.5	PAD Statistics	12
1.6	PAD Risks Ratio	13
1.7	Classification of PAD	14
1.8	Atherosclerotic Lesions of PAD	15
1.9	Bypass Surgeries of PAD	17
1.10	Various Routes of Blood Flow	19
1.11	Revascularization Techniques	21
1.12	Current Retroperfusion Surgery Compared to Standard Bypass Surgery	23
1.13	Arteriovenous Manipulations Comparisions	24
3.1	Theoretical circuit of the experimental setup.	33
3.2	Locations explored during ex-vivo experiments.	35
3.3	Catheter configuration of the experimental setup.	36
3.4	Animal Setup	38
3.5	Catheter configuration of the experimental setup.	40
3.6	Microsphere Negative Pressure Filtration System	43
3.7	Muscles of perfusion interest.	46
4.1	Guidewire in Ex-vivo Dog Foot	49
4.2	Ex-vivo Locations	50
4.3	Ex-vivo Pressure Flow Data	51
4.4	Ex-vivo Linearized Pressure Flow Data	52

Figure Page

4.5 In-vivo Pressure Flow Data 54
4.6 Ex-vivo and In-vivo Pressure Flow Data Comparison 55
4.7 Arteriogram and Venogram at Popliteal Bifurcation. 56
4.8 Microsphere Perfusion Territory Data 60
4.9 Blood Gas Data 61
5.1 Early Ex-vivo Retroperfusion Test 66
5.2 Early In-vivo Test of Retro Access 67
5.3 Distal Shunting Effects of Flow 68
5.4 Distal Pressure at Popliteal Vein Bifurcation 69

ABSTRACT

Kemp, Arika D. M.S.B.M.E., Purdue University, December 2014. Peripheral Venous Retroperfusion: Implications for Critical Limb Ischemia and Salvage. Major Professor: Ghassan S. Kassab.

Peripheral arterial disease is caused by plaque buildup in the peripheral arteries. Standard treatments are available when the blockage is proximal and focal, however when distal and diffuse the same type of the treatment options are not beneficial due to the diseased locations. Restoration of blood flow and further salvaging of the limb in these patients can occur in a retrograde manner through the venous system, called retroperfusion or arteriovenous reversal. Retroperfusion has been explored over the last century, where early side to side artery to venous connections had issues with valve competency prohibiting distal flows, edema buildup, and heart failure. However, more recent clinical studies create a bypass to a foot vein to ensure distal flows, and though the results have been promising, it requires a lengthy invasive procedure. It is our belief that the concerns of both retroperfusion approaches can be overcome in a minimally invasive/catheter based approach in which the catheter is engineered to a specific resistance that avoids edema and the perfusion location allows for valves to be passable and flow to reach distally. In this approach, the pressure flow relations were characterized in the retroperfused venous system in ex-vivo canine legs to locate the optimal perfusion location followed by in-vivo validation of canines. Six canines were acutely injured for 1-3 hours by surgical ligation of the terminal aorta and both external iliac arteries. Retroperfusion was successfully performed on five of the dogs at the venous popliteal bifurcation for approximately one hour, where flow rates at peak pressures reached near half of forward flow (37±3 vs. 84±27ml/min) and from which the slope of the P/F curves displayed a retro venous vasculature resistance that

was used to calculate the optimal catheter resistance. To assess differences in regional perfusion, microspheres were passed during retroperfusion and compared to baseline microspheres passed arterially prior to occlusion in which the ratio of retroperfusion and forward perfusion levels were near the ratio of reversed and forward venous flow (0.44) throughout the limb. Decreases in critical metabolites during injury trended towards normal levels post-retroperfusion. By identifying the popliteal bifurication as a perfusion site to restore blood flow in the entirety of the distal ischemic limb, showing reversal of injury, and knowing what catheter resistances to target for further chronic studies, steps towards controlled retroperfusion and thus more efficient treatment options can be made for severe PAD patients.

1. INTRODUCTION

1.1 Background

1.1.1 Cardiovascular System

The human need for a cardiovascular system is the result of being a multi-dimensional, multi-cellular organism [1]. Diffusion, the movement of ions, gases, or small molecules down their concentration gradient, and convection, the movement of water and solutes across a membrane by a transmembrane pressure gradient, are the basic mechanisms a single cell needs to stay alive. However, when an organism is or becomes more complex in size and number of cells, molecular concentration will decrease as the distance increases as defined by Fick's Law of Diffusion [2]. Therefore the mechanism at which a cell receives and delivers its nutrients and wastes, respectively, requires a more efficient delivery system.

The cardiovascular system has evolved into a very efficient delivery system due to the major branching that occurs. Cells can easily obtain their nutrients when the diffusion distance is no longer an issue. The fluid which brings the nutrients and waste to and from the tissue, requires flow so cells can continue to receive fresh new nutrients, and wastes can be properly disposed. The movement of blood is largely due to the pumping action of the heart. As the heart pumps, it creates a necessary pressure gradient for the blood to circulate throughout the body via the major branching [3]. The anatomy and physiology of circulation, and the mechanics of blood flow are further discussed.

1.1.1.1 Anatomy and Physiology

Different parts of the cardiovascular system have unique structures, functions, and properties. The basic components are the heart, vessels, and blood. The heart acts as a pump to distribute the transport medium, blood, throughout the body through conduit-like vessels. The circulation of blood is critical for cell survival because it contains nutrients and oxygen needed for energy production and metabolism [1].

The cardiovascular system can be broken up into two subsystems, the pulmonary and systemic. Figure 1.1 shows the pulmonary circulation occurring between the right and left heart; this circulation is necessary for gas exchange to occur. When the oxygen-poor blood reaches the right side of the heart through either the superior venae cavae from upper body and brain, or the inferior venae cavae from the lower body, it is then pumped into left or right lung via the pulmonary artery. The waste gas, carbon dioxide, that the cells gave off during circulation is released and further exhaled whereas oxygen, obtained from inhalation, is picked up by the red blood cells for redistribution throughout the body. The now oxygen-rich blood returns to the left side of the heart via the pulmonary veins where it is then further pumped out to the rest of the body by the systemic circulation.

Once the oxygen-rich blood is pumped out of the left heart it reaches the systemic circulation where the largest artery, the aorta, branches to the upper body and brain and then further descends past the heart to reach the lower body. Both the upper and lower body receive oxygen-rich blood via the same route: beginning at an elastic artery, followed by branching into muscular arteries and further into smaller arteries called arterioles, and again to capillaries where the appropriate gas and nutrient exchange occurs over a large cross sectional area. The now oxygen-poor blood is received by the venules which collectively pool into veins that eventually reach the right heart via the venae cavaes. This cycle of circulation repeats continuously where each component is uniquely structured to its function.

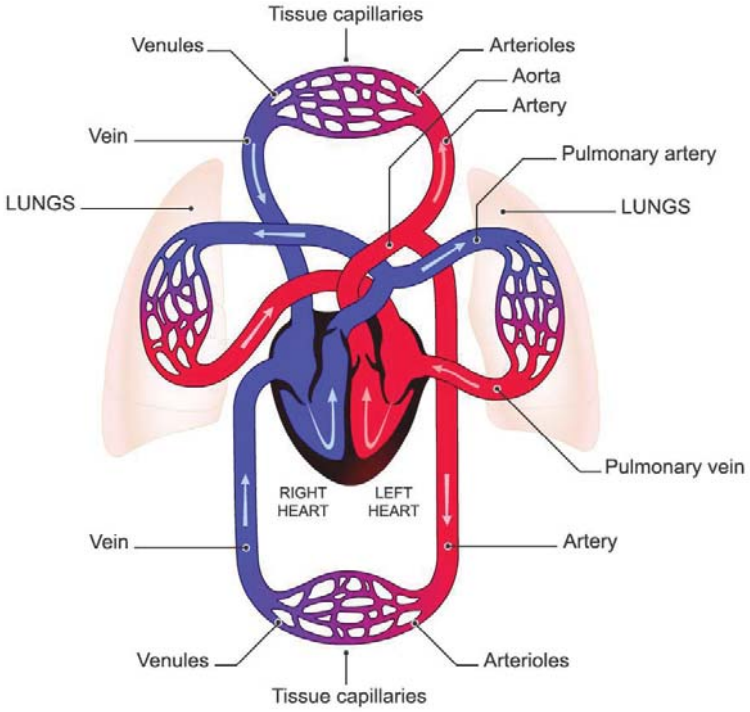

Fig. 1.1. This figure shows a basic schematic of the cardiovascular system. [4]

1.1.1.2 Vasculature Components

All blood vessels move blood throughout the body, however each blood vessel type has unique structures and properties. Most blood vessel types have three distinct layers: an inner layer called the tunica intima, a middle layer called the tunica media, and an outer layer called the tunica externa (Figure 1.2). The innermost layer comprises of an endothelial layer and a basement membrane plus an additional internal elastic layer in arteries [5]. The medial layer is comprised of mostly smooth muscle cells and additional elastic layer for arteries [5]. The outermost layer, or the adventitia, is mainly composed of collagen, elastin, and other interconnective fibers of the extracellular matrix [5]. Though both arteries and veins contain all three layers in general, capillaries only have a tunica intima [5].These structural differences correspond with their respective function.

Arteries are mainly in charge of the delivery of blood from the heart whereas veins are responsible for the return of blood to the heart and capillaries see to the exchange of nutrients and waste [5].

Because arteries are the first vessels in line to receive the high pressure oxygen-rich blood, they have a unique composition that permits their function. Figure 1.2 shows a thick medial section. This medial section is mainly comprised of smooth muscle cells and is responsible for vessel contraction. Vessel constriction occurs particularly at the arteriole level which allows capillaries to have a controlled input pressure. Though large vessels constrict as well, due to the increase in cross sectional area from arterioles, their contribution to flow regulation is greater. The regulation of pressure at the capillary level is critical for proper exchange to occur even at times of elevated pressure, due to standing or exercise, or lowered pressure, due to sleeping, of which the arteriole would contract or dilate, respectively [1].

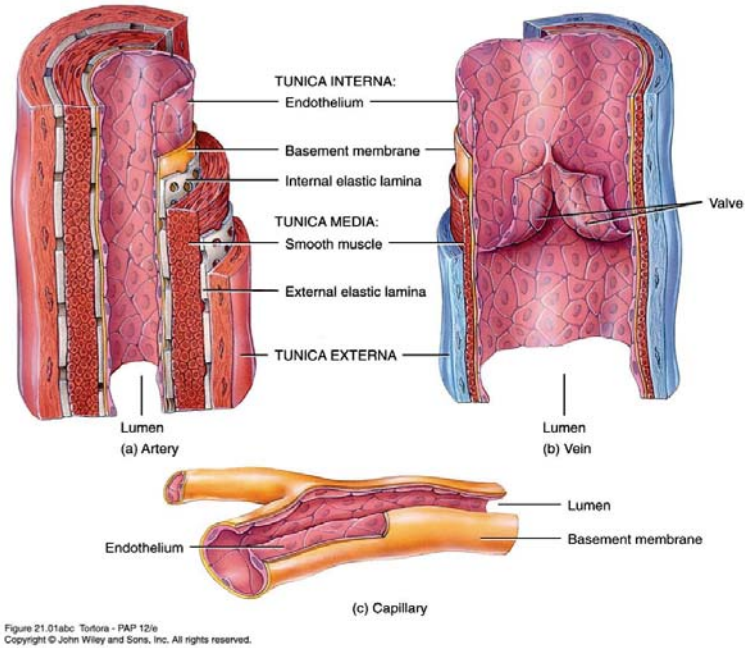

Fig. 1.2. This figure shows the structures of an artery, vein, and capillary blood vessel. [6]

The vasculature pressure dynamics are shown in Figure 1.3. It is clear that the major pressure drop occurs in the arteries, but conversely little to no pressure drop occurs across the venous portion of the circulation pathway. Therefore, the assumption that veins' function do not pertain to maintenance of pressure would be true, where Figure 1.2 reveals that veins have a much thinner medial layer. Figure 1.2 also depicts a valve within the lumen of the vein attached to the endothelial layer. Valves are necessary for veins to return blood back to heart due to the oxygen-poor blood flowing against gravity. Besides efficient blood return to the heart, veins also take a role in blood storage, in which nearly 70% of all resting blood volume resides in the venous system [3], which is why they are occasionally referred to as capacitance vessels [1]. Veins are very compliant which contributes to their distention in increased pressures, when transmural pressure increases from 0 to 10mmHg the volume is increased by 200% to combat the increase in pressure [1].

Although the movement of blood is important, the original purpose of blood is to act as a transport medium for cells to obtain nutrients and oxygen and release waste and carbon dioxide. The site at which this delivery and return is at the capillary level. Figure 1.2 reveals the structure of a capillary which, as previously mentioned, only contains the inner most blood vessel layer, the tunica intima. Similiarly, as to arteries and veins, a capillary's structure largely corresponds to its function.

After the blood reaches the arterioles, a large branching network forms, and the blood is dispersed into a capillary bed of large surface area. Due to a capillary's size compared to other blood vessels ($\sim 1\mu m$) and the circulatory system being a closed circuit (i.e. flow rate is constant), Equation 1.1 expresses what ultimately occurs at a capillary. Because the flow rate (Q) is constant and the cross sectional area (A) of a capillary is very small, the velocity (V) will dramatically decrease at the capillary level. Combining all these characteristics, maximum oxygen and nutrient exchange will take place by cause of the large amount of area and slowed speeds [1]. How exchange happens is explained into further detail of the microcirculation.

$$Q = VA, \tag{1.1}$$

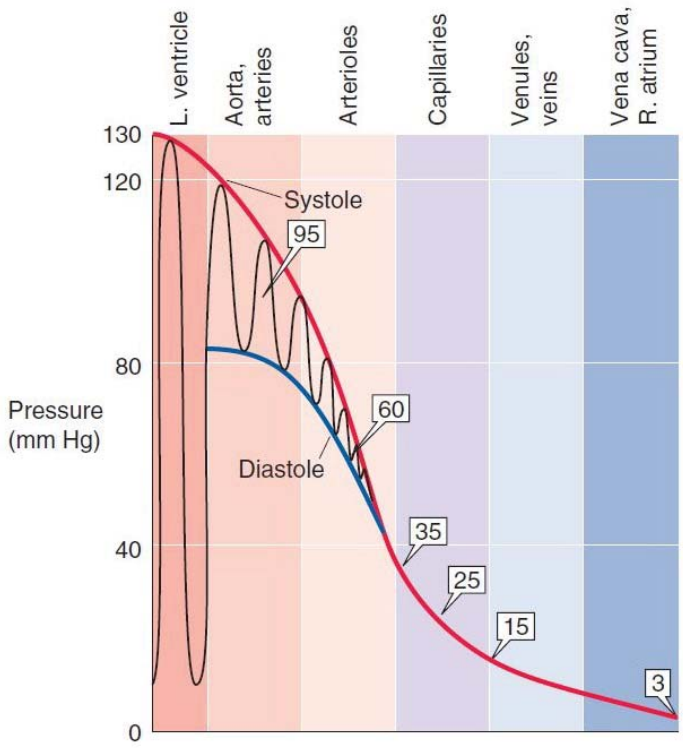

Fig. 1.3. This figure shows the pressure dynamics of the vasculature. [1]

1.1.1.3 Microcirculation

The movement of blood in the smallest blood vessels is done by the microcirculation. The role of arterioles, as previously mentioned, are to control the input pressures to a capillaries, because of this crucial function arterioles are also known as "resistance vessels". By contracting when exposed to high pressure levels, the cross sectional area decreases and thus the resistance increases. The Hagen-Poiseuille relationship (Equation 1.2) easily shows how a decrease in cross sectional area results in a large increase in resistance and thus a larger pressure drop before entering the capillaries (1.3) [7].

$$R = \frac{8\pi\mu l}{(CSA)^2}, \tag{1.2}$$

$$\Delta P = QR, \tag{1.3}$$

Although pressure maintenance before entering capillaries is critical for proper exchange to take place, various other parameters also factor into efficient exchange. The net movement of fluid in capillaries, or "exchange vessels" is governed by Starling's Equation.

$$J = L([P_c - P_i] - \sigma[\pi_c - \pi_i]), \tag{1.4}$$

In summary, the net fluid movement (J) is equal to the difference of fluid filtered out in the tissue and fluid reabsorbed back in the blood stream. The P and π terms indicate the hydrostatic pressure and oncotic pressures, respectively, and c and i, capillaries and interstitial space, respectively. L is the conductivity constant dependent on the permeability and surface area of the capillary and σ represents the idealness of protein movement across the membrane (typically 1 for plasma proteins) [1].

The hydrostatic pressure of the capillaries is equivalent to the inlet pressure of blood whereas of the interstitial space it is the tissue pressure acting on the capillaries. Here, the usual laws of diffusion are overshadowed by the presence of hydrostatic pressure [8]. Oncotic pressure represents the driving force of fluid due to protein concentration. E.g. the force of entering blood pushes fluid out into tissue, however this results in an increase of protein concentration left in the blood. This higher oncotic pressure then drives the reabsorbance of fluids at the venule end of the capillary [1]. Figure 1.4 explains how these terms interact as the blood travels through a capillary from arteriole to venule end. Initially, a net filtration will occur at the arteriole end, but as the blood reaches the venule end a net absorption occurs. Overall, the initial filtrate and final reabsorbate result in a slightly positive net filtration in a healthy individual [1].

The apparent redundancy of filtering and reabsorbing is because the contents of what is being filtered out are the nutrients and oxygen on the arteriole side versus what is being reabsorbed back in is the waste and carbon dioxide on the venule side of the capillary bed. Besides collecting the oxygen poor blood from the capillaries,

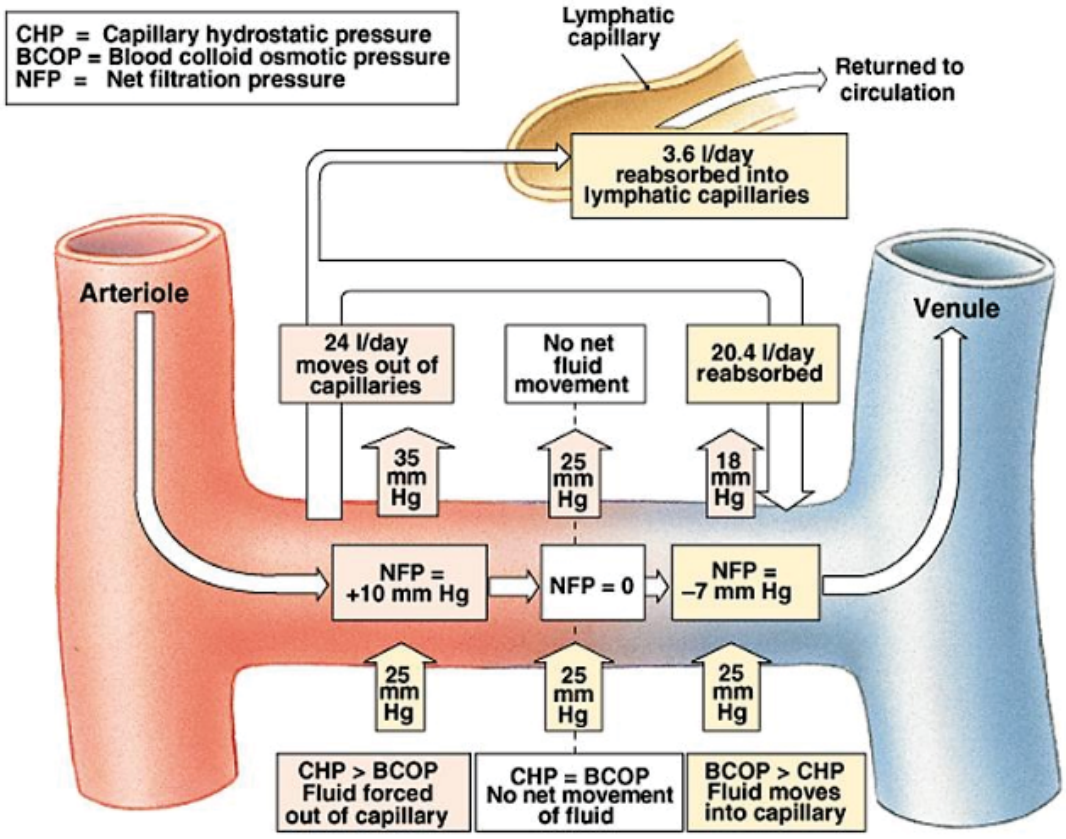

Fig. 1.4. This figure shows the driving forces acting on a capillary. [9]

venules also have some filtering functions themselves. Often, white blood cells escape from venules to reach the tissue to fight infection [1].

How the blood travels throughout the macro- and microcirculation have been explained to great detail, but as to what causes the blood to move, is discussed in the following hemodynamic's section.

1.1.1.4 Hemodynamics

Flow dependencies can be explained by Equation 1.5 where the nature of blood flow or hemodynamics is expressed by this simple relationship between ΔP, a pressure difference, and R, a resistance of what the blood is flowing through [7].

$$Q = \Delta P/R, \tag{1.5}$$

Blood circulation requires a pressure difference to be present, as indicated in Equation 1.5. The major pressure difference in the cardiovascular system occurs in the heart, between the aortic root and the right atrium, this difference propels blood throughout the body. When blood leaves the left side of heart, the oxygenated arterial blood is approximately 100 mmHg (i.e. mean arterial pressure) and when the blood returns to the right side of the heart, the deoxygenated is approximately at 5 mmHg [7]. This resulting pressure difference drives blood circulation in multi-cellular, multi-dimensional organisms.

The pressure difference that occurs systemically, can also be explored locally. Starling's Equation showed the importance of a pressure difference at a capillary level for filtration. At each location along the capillary there is a balance of pressures taking place resulting in either filtration or reabsorption, but if the pressures equal there will be no net movement of fluids i.e. no driving force for flow occur. And in a broader aspect, the hydrostatic pressures at each end of the capillary need to differ for blood to actually flow through the capillary and for adequate exchange to occur, respectively. The former is governed by Equation 1.5 and the latter is governed by Starling's Equation 1.4.

Although the cardiovascular system has evolved into a reasonably complex system for multicellular multidimensional organisms, there are various locations in which the system can be perturbed and lead to a disease state. Relevant diseases that can take place are discussed in detail.

1.1.2 Disease

Although the mechanistic nature of the cardiovascular system is fairly straightforward, there are various ways for the system to become disrupted. The pumping action of the heart can begin to fail due to stress from high pressures or become weak due to overcompensation of an increased workload [1]. The transportation of blood can become less streamline due to changes in pressures or areas of narrowed flow [10]. The blood itself can become contaminated leading to adverse effects on the endothelial layer of the vessels and thus decrease its ability to properly nourish the body. [10] Because the components of the system are interconnected, when one component fails for any reason it largely affects the other components as well. There are countless ways for the system to be disrupted, and for this investigation the disease of interest begins with the blood components itself.

1.1.2.1 Development

Blood is the transport medium of the body, and once it becomes contaminated, just like the water supply to a house, it can cause corrosion of the pipes and eventually, if not taken care of, the plumping will fail altogether and water will have no way to travel. This concept of contaminated water leading to pipe corrosion and disruption of water supply is analogous to blood and the body. When blood becomes contaminated it can cause endothelial dysfunction (inner most layer of a vessel) and through a series of steps lead to reduced blood flow [10]. Each stage of this progression is discussed.

The toxins that contaminate blood and begin to destroy the endothelial layer of blood vessels can come from different origins. From food intake to smoking habits, someone's diet and lifestyle can largely attribute to cardiovascular disease. The major irritants include low density lipoproteins (LDLs), toxins from smoking, and high blood pressure [11].

1.1.2.2 Plaque Formation

When the blood has increased levels of these irritants, the blood vessel's inner most wall begins to dysfunction [11]. As the endothelial layer starts to break down due to overexposure of these toxins, it is thought that the LDLs move in between the inner and medial layer, literally making the blood vessel 'fatty'. In an attempt to protect the vessel, macrophages try to uptake the LDLs, but the result is a toxic macrophage, called a foam cell [11]. LDLs continue move in between the inner and medial and eventually form a 'fatty streak' in the blood vessel. As the fatty layer continues to attract more fats and lipids, this triggers smooth muscles from the medial layer to migrate into the fatty streak in an attempt to form a fibrous cap [11]. This fibrous cap results in an overall smaller cross sectional area and thus reduced blood flow.

1.1.2.3 Blockages

The fibrous cap that results from plaque buildup can eventually block off the artery entirely, form a clot, or a piece may break off [11]. Whatever the case, the result is massive reduced flow in the artery past or distal to the plaque site or from the traveling clot/plaque getting lodged in a smaller artery. This massive flow reduction will cause the tissue distal to the blockage to become ischemic, short of oxygen and necessary nutrients, and, if prolonged, necrotic, die.

1.1.2.4 Atherosclerosis

Blockage or partial blockage and hardening of arteries due to plaque buildup is called atherosclerosis [5]. Atherosclerosis mainly occurs in large and medium sized arteries and depending on where these arteries are located can be detrimental [5]. When blood flow is largely reduced, ischemic and necrotic tissue are the eventual result. Locations at which the flow is particularly sensitive include coronary, carotid, renal, and peripherial arteries [5].

Reduced flow in these arteries causes the specific diseases of coronary artery disease, carotid artery disease, chronic kidney disease, and peripheral arterial disease. Major blockage in each disease results in a heart attack, stroke, kidney failure, and ulcers (minor tissue death) or gangrene (major tissue death), respectively cite.

The latter of all diseases that may develop from atherosclerosis, is described in detail in the following section.

1.1.3 Peripheral Arterial Disease

Peripheral arterial disease, or PAD, is the specific disease of developed atherosclerosis in the periphery. It affects 8 to 12 million Americans, where American men and women in the sixties age group have a 5% prevalence, and the prevalence increases to 10% and 20% as the age group moves to the seventies and eighties (Figure 1.5) [12,13].

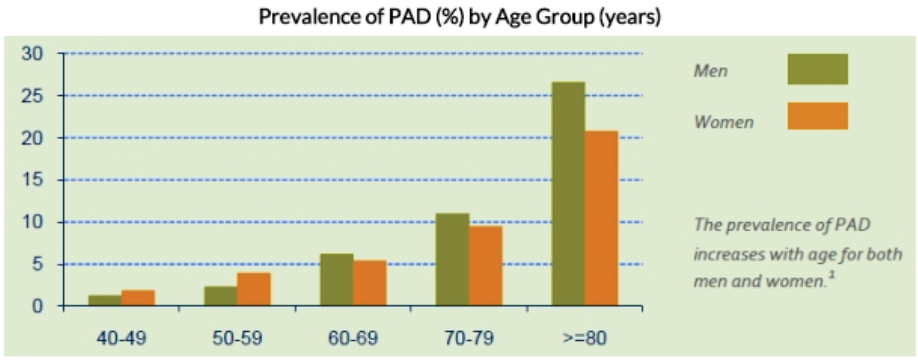

Fig. 1.5. This figure shows the statistics of peripheral arterial disease according to CDC [13].

1.1.3.1 Risk Factors

Those susceptible to PAD is a combination of controllable and uncontrollable risk factors. Some of these risk factors include smoking, obesity, diabetes mellitus, low physical activity, high cholesterol, and high blood pressure. As previously mentioned,

age is also a factor, as well as gender and ethnicity. These risk factors are displayed in a odds ratio in Figure 1.6 where a male is 1 to 2 times more likely at risk for PAD [10].

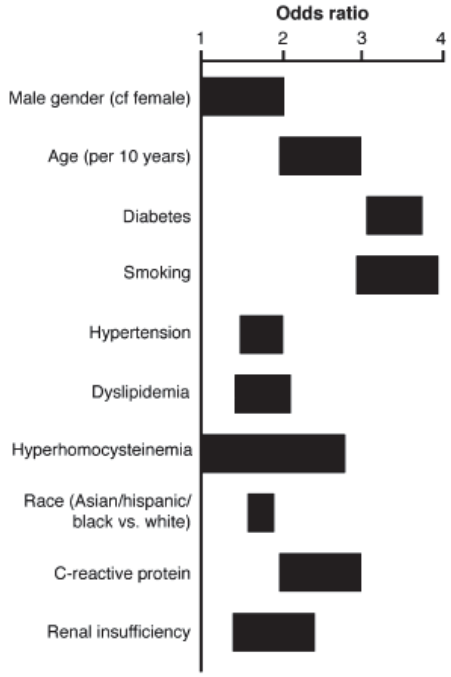

Fig. 1.6. This figure shows the risks of peripheral arterial disease ([10]).

Even though there is a list of risk factors for PAD, the development of the disease is equivalent to the process described for atherosclerosis, but located in the periphery, particularly the legs.

1.1.3.2 Progression of PAD

Throughout PAD, blood flow is reduced in the periphery more and more due to continual plaque buildup on the arterial wall. Initially, there is little to no symptoms of the disease, but as the disease progresses pain during exercise, or claudication, is experienced. As claudication becomes worse, the walking distance of the standard 6-minute walking test become very short before claudication sets in and eventually pain

is experienced even during rest [14,15]. In the most severe stages of PAD, minor tissue lose can cause sores or skin ulcers due to ischemia and later, if the lack of blood flow covers large areas, gangrene can set in and result in major tissue loss. The progression of PAD has been previously classied into Fontaine's Stages, but more recently has been broken up into grades and categories by Rutherford (Figure 1.7) [10].

Fontaine		Rutherford		
Stage	Clinical	Grade	Category	Clinical
I	Asymptomatic	0	0	Asymptomatic
IIa	Mild claudication	I	1	Mild claudication
IIb	Moderate to severe claudication	I	2	Moderate claudication
		I	3	Severe claudication
III	Ischemic rest pain	II	4	Ischemic rest pain
IV	Ulceration or gangrene	III	5	Minor tissue loss
		III	6	Major tissue loss

Fig. 1.7. This figure shows the classification of peripheral arterial disease in the old Fontaine stages and new Rutherford categories [10].

Typical clinical assessments include palpation and auscultation of the foot, an ankle-brachial index (ABI) in which the ratio of ankle pressure to arm pressure is made (normal is 1.00-1.39 and abnormal is <0.90), a 6 minute walking test, as previously mentioned, as well as a treadmill test in which the patients is exercised until the onset of symptoms [14–16]. If the pain experienced during exercise is subsided during rest, the patient is considered to have intermittent claudication. However, if the pain does not subside during rest, the patient is considered have the most severe form of PAD, critical limb ischemia (CLI) [16]. Various types of atherosclerotic lesions can contribute throughout PAD and at each of these specific subdivisions.

1.1.3.3 Atherosclerotic Lesions

Blockages are most likely to occur in the aortoiliac segment (suprainguinal region) or the femoral-poplital segment (infrainguinal region), shown in Figure 1.8. The suprainguinal region is more proximal, more risky to treat, but has the best treatment outcomes ($\sim 90\%$ patency after 5 years). The infrainguinal region is more distal, less risky to treat, but 5 year patency is $\sim 70\%$ [10].

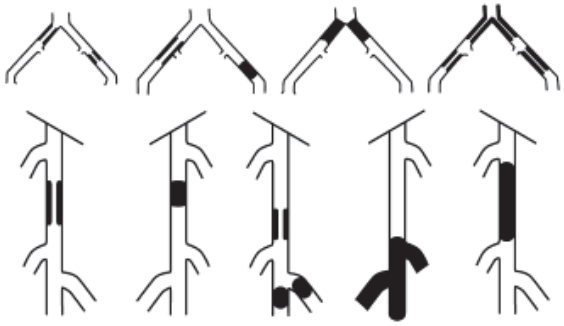

Fig. 1.8. This figure shows the various atherosclerotic lesions of peripheral arterial disease with the first row aorto-iliac lesions and the second row fem-popliteal lesions [10].

As opposed to typical focal and proximal blockages, patients with CLI and diabetes are more likely to have diffuse and distally located lesions [10].

1.1.3.4 Treatment Options

Since the main indicator of PAD is claudication, the one who experiences this pain must be educated enough to know the origin of their pain. Typically, those who experience claudication do not recognize that their pain is specifically muscle pain caused by the reduced blood flow. This reduction in blood flow limits the amount of oxygen available for the muscles. Muscles need more oxygen when more work is being done, i.e. more exercise equals more work. However, due to the older age group that PAD is present in, they may think that their pain is due to old age and

their deteriorating joints or because PAD has a large overlap with other diseases such as diabetes their pain can be mistaken for nerve pain or neuropathy (common in diabetics) [17].

Because PAD has a silent progression, treatment options are critical for each stage of the disease, particularly the late stages. Initial treatment options include medications to treat risk factors (high blood pressure and high cholesterol), improve walking distance (cilostazol and pentoxifylline), and/or antiplatelet activation (aspirin, Plavix) [10].

If medication proves to not be enough and the plaque buildup has not yet fully blocked an arterial segment, minimally invasive procedures such as angioplasty and/or stent placement is considered. Angioplasty is a common cardiovascular procedure in which a catheter is inserted to the area of interest and a balloon is inflated to temporarily re-open the narrowed artery. To keep the artery open, the same procedure takes place, but a stent is also released once the balloon is inflated to re-open the artery longer than angioplasty could itself [10].

Once the plaque buildup has led to a full block in blood flow, bypass surgeries are considered. The grafts used for bypass are mostly accessory veins from the patient. Synthetic grafts can be used but the patency statistics are continuously much less and therefore unfavored [10]. Figure 1.9 shows typical artery to artery bypass surgeries that take place in focal and proximal lesions.

A couple other later stage treatment options include endoarterectomy, where the plaque is surgically removed, and catheter directed thrombolysis, where a specialized catheter is used to scrape and remove the plaque buildup [10]. Although there are other late stage treatment options, bypass surgeries are considered 'the gold standard' for PAD.

Like previously mentioned, PAD patients with CLI and diabetes are more likely to have diffuse and distal occlusions rather than focal and proximal. These mentioned treatment options are only feasible for the latter, leaving the former without a common

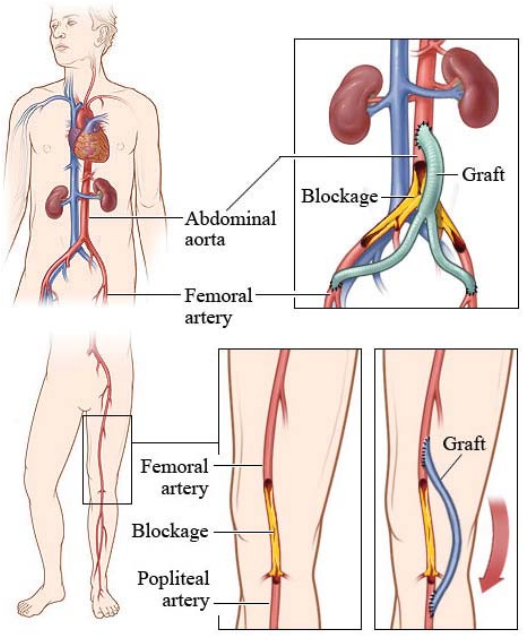

Fig. 1.9. This figure shows an aortobifemoral bypass and a femoropopliteal bypass that typically take place in later stage PAD patients [18].

treatment option. Often times, failed treatments and CLI patients are left with the only treatment option of amputation [10].

Although PAD patients with diffuse and distally location occlusions have no common treatment option, unique revascularization techniques have been explored, particularly retroperfusion.

1.1.4 Retroperfusion

The common pathway for blood begins in the lung to left heart to artery to arteriole to capillary to venule to vein to right heart to finish again in the lung. Once reduced flow occurs in an artery, less nutritive blood can make it to the microcirculation, leaving the previously supplied tissue now in need of oxygen and nutrients. In the previously described bypass surgeries the blood is rerouted to travel from an

artery to the graft to distal patent artery as the process continues. For retroperfusion the blood flow now has different pathways it can take.

For more than a hundred years, attempts have been made to explore a new blood pathway both clinically and experimentally [19]. Rather than the previously mentioned forward route, from artery to vein, exploration of the undiseased reverse route was considered for revascularization of an ischemic area. Since the venous system is unaffected by even the most severe atherosclerotic diseases, it provides an ideal conduit for blood flow. Various efforts of arteriovenous reversal were explored, but the main idea fell in two categories, in-situ venous connection and excised venous graft. This new blood pathway would began at the most distal satsifactory artery which is then connected surgically to a nearby vein, or an accessory vein was grafted to a distal vein, in which the blood now has a few flow options. Ideally the flow would reach the venule level and then to the capillary in this reverse route, but collaterals could form between the newly arterialized veins and native vessels in sort of a natural grafting process, or the flow could be immediately diverted or shunted to a native venous collateral and completely bypass the microcirculation [20]. This shunting effect was explained by Heimbacker in 1950 along with a demonstration of oxygen uptake in reverse perfusion [21]. Additional proof of reverse route exchange was done by Zweifach in 1940 when he showed reversed venous blood resulted in colloidal dye to pass along the entire length of the capillary network [8]. Figure 1.10 depicts the differences of blood routes in a normal case, an occluded case, standard bypass treatment, and retroperfusion.

1.1.4.1 History

Experimental investigation of this new revascularization technique has been driven by the portion of PAD patients that do not benefit from conventional surgical techniques of which primarily target proximal and focal occlusions. Beginning just prior to the 19th century, retroperfusion was considered greatly in cardiac revascularize-

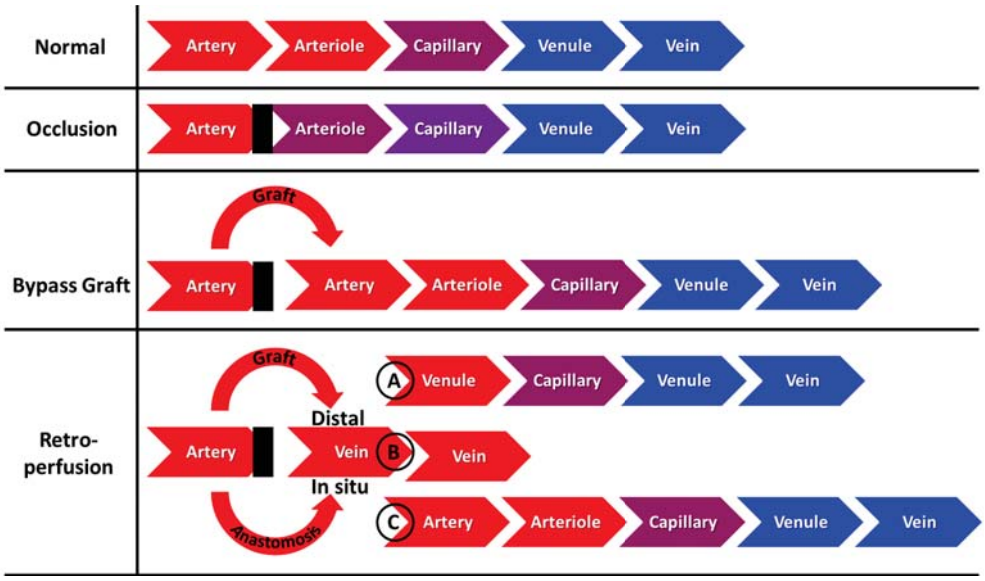

Fig. 1.10. This figure shows the various routes of blood starting from a normal route, a occlusion (black block represents an occlusion), standard bypass treatment, and retroperfusion techniques of grafting to a distal vein and surgically attaching an in-situ vein and then the various routes the blood can take from there. A represents the theoretical and ideal flow of the blood, B represents the blood finding a native venous collateral and shunting back to the heat, and C represents the collaterizations occuring between the newly arterialized veins and native arteries.

tion [22] and then in the periphery by 1912 [23]. Early experiments of arteriovenous manipulation was not the result of retroperfusion entirely, but creation of a fistula (AVF), in which a surgical connection was made directly at the artery end and the venous end [24]. This encouraged other investigators to explore arteriovenous reversal (AVR) a few years after, but went in and out of popularity due to inconsistent results and failed expectations, theoretically, experimentally, and clinically [23–25].

Due to the success being unpredictable and major critical reviews, AVR was left unexplored for nearly 40 years [24]. Its revival was in 1949 by Leger in Paris once heparin became available [24, 26]. Jordan and Johnston also described success with AVR the same year [19], which led to optimistic clinical trials. However, Szilagyi had

9 clinical trials that all led to major failure due to valve obstructions preventing the arterial blood in the retro venous system from reaching the distal limb [19]. Various innovative attempts for revascularization followed of which all failed. One particular study in 1959 tried to use similar concepts in a typical bypass by use of an in-situ venous graft with valve destruction, in which the great saphenous vein (GSV) was connected to the femoral artery and distal end to a patent artery to allow the GSV to be left in its natural subcutaneous bed, but major branching and shunting from the arterialized vein resulted [27]. This shunting effect was overcome by recognition of the valve locations. Certain valves, valves in perforating veins, are oriented to drain from superficial to deep and prevent deep flow reflux into superficial veins, thus if flow is in the superficial system it can easily be shunted directly to the deep and completely bypass the microcirculation [27]. The recognition of valve orientation was a key component in early AVF and AVR studies.

Despite the issues, the intense collateral formation and high blood flow at arteriovenous sites were enough to encourage investigators to continue exploring arteriovenous revascularization techniques. A second AVF was put in the extremity in 1976 by Lavigne, only to observe that an additional AVF resulted in left ventricular strain and ultimately heart failure, a decrease in flow through the more proximal fistula, and a decrease in perfusion distal to the fistula, thus displaying the limitations of arterio-venous fistulaes [28]. Johansen and Bernstein in 1979 [25], showed their success with arteriovenous reversal in canines once they had a reliable irreversible injury in which they could ensure native collaterals were not the result of improved flow. When a full venous reversal from femoral artery to vein (AVR) was made, the dogs had nearly immediate life-threatening massive edema. To avoid this, a second group of dogs had an end to side connection from femoral artery to vein (arteriovenous anastomosis, AVA) for one week and then a full venous reversal. Their second group of dogs avoided massive edema but could not confirm retrograde perfusion of the terminal circulation.

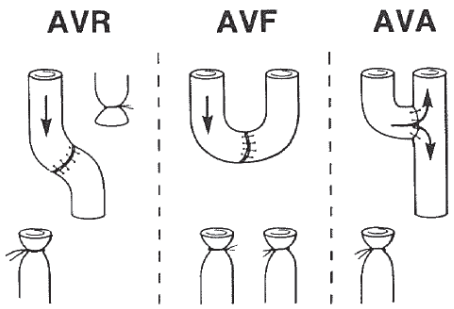

Fig. 1.11. This figure shows the revascularization techniques explored in arteriovenous manipulations, arteriovenous reversal (AVR), arteriovenous fistula (AVF), and arteriovenous anastomosis (AVA) [24].

Gerard led an acute retroperfusion experiment in 1981 that explored the differences between AVF, AVR, and AVA (arteriovenous anastomosis) shown in Figure 1.11. His results indicated AVR could be successful if the reversal takes place as distally as possible [24].

Graham and associates ran with AVR in 1983 [29], but looked at the popliteal level for perfusion to test whether flows here could surpass any native venous valves and reach more distal than ever. Flows were shown to reach more distal in their experiments. From microsphere injections, they were able to indicate that distal limb levels were perfused primarily by the reverse venous flow whereas proximal limb levels suggested supply by stimulation of intense collateralization. To further investigate the collaterals formed, the same group later proved through assessment of tissue oxygenation and absence of tissue necrosis that these new vessels provided nutritive flow to the ischemic limb [30].

As the Graham group led into the discovery of the mechanism for revascularization [31], other investigators explored in situ venous anastomosis less and vein graft removal more which Lengua in 1975 showed success [32]. With the venous graft now excised its distal end could anastomose at the foot to ensure flow distally as opposed to in situ when the perfusion site was more proximal and less distal flow was observed.

More recent clinical trials of retroperfusion have used bypass for distal venous arterialization [33–36], brought about by Lengua's long-term outcome report in 1995 [37], and their results have been promising. The current technique is similar to standard bypass but the distal connection is made with a foot vein rather than the nearest patent and undiseased artery; the differences are depicted in Figure 1.12. The graft of choice, similar to standard bypass procedures, is the patient's great/long saphenous vein [33–36]. In some cases, the graft was harvested in situ like earlier retroperfusion experiments [36], but in order to avoid venous-venous shunting and valve dampening for distal flow, the vein was exposed cranially up to proximal anastomosis site with all tributaries ligated, and all valves stripped out with a valvulotome or other cutting device [33–36], respectively. Other times, the bypass was made as short as possible so that the distal portion of the saphenous vein could remain and the valves were either stripped or the graft was anastomosed in reverse [33, 34]. One group even ligated the great saphenous vein to prevent any major shunting that in return causes high cardiac output and thus heart failure [38]. The proximal anastomsis was always between the most distal satisfactory artery and the proximal end of the vein. The distal anastomosis was made at to either the dorsal venous arch or the medial malleolus vein. This distal attachment now allows flow directly to the foot, surpassing issues with distal flow. The overall limb salvage rates were between 83 and 92% [33–36].

1.1.4.2 Limitations

The limitations of retroperfusion fall into two categories, those that used in-situ venous reversal and those that used excised venous grafting for flow reversal. The advantages and disadvantages of each are depicted in Figure 1.13.

1.1.4.2.1. In-situ Retroperfusion

The hopefulness and issues with in-situ retroperfusion initially rose from arteriovenous fistulas when high flow rates and undeniable collaterizations formed at the

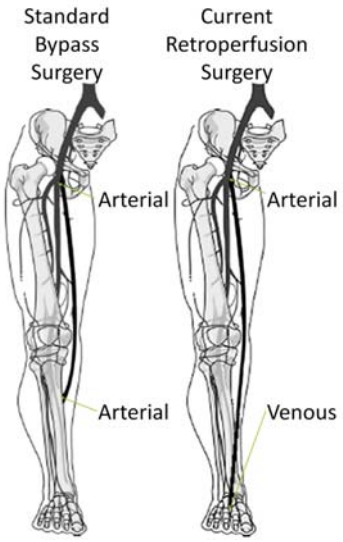

Fig. 1.12. This figure shows the current retroperfusion surgery compared to standard bypass surgery [10].

surgical connection between the artery and vein which allowed the nearby tissue to survive. However, distal flows were not met and often amputation was still needed or if the patients had developed heart failure from the resulting high cardiac output some died [24]. AVRs then came into focus, but the large arterial pressures now being directed in the venous system was too much for the thin vessels and massive edema resulted [25]. Pre-conditioning of the venous system followed as AVAs were used with or without AVR following to avoid excessive edema, however proximal connections at the femoral level had the venous valves obstructing the flow before reaching distal portions [24,25]. Distal connection, at the popliteal level led to distal flows in foot [29,30], but then the focus shifted from the actuality of the technique (did limb salvage take place) to mysteries of the technique and thus time was then spent on the mechanistic feature of collaterization rather than further validation of the reversal site [31]. From our research, the only clinical results from the last AVR technique resulted in upper extremity salvage [39] and large-area foot skin retrograde avulsion [40], but no limb

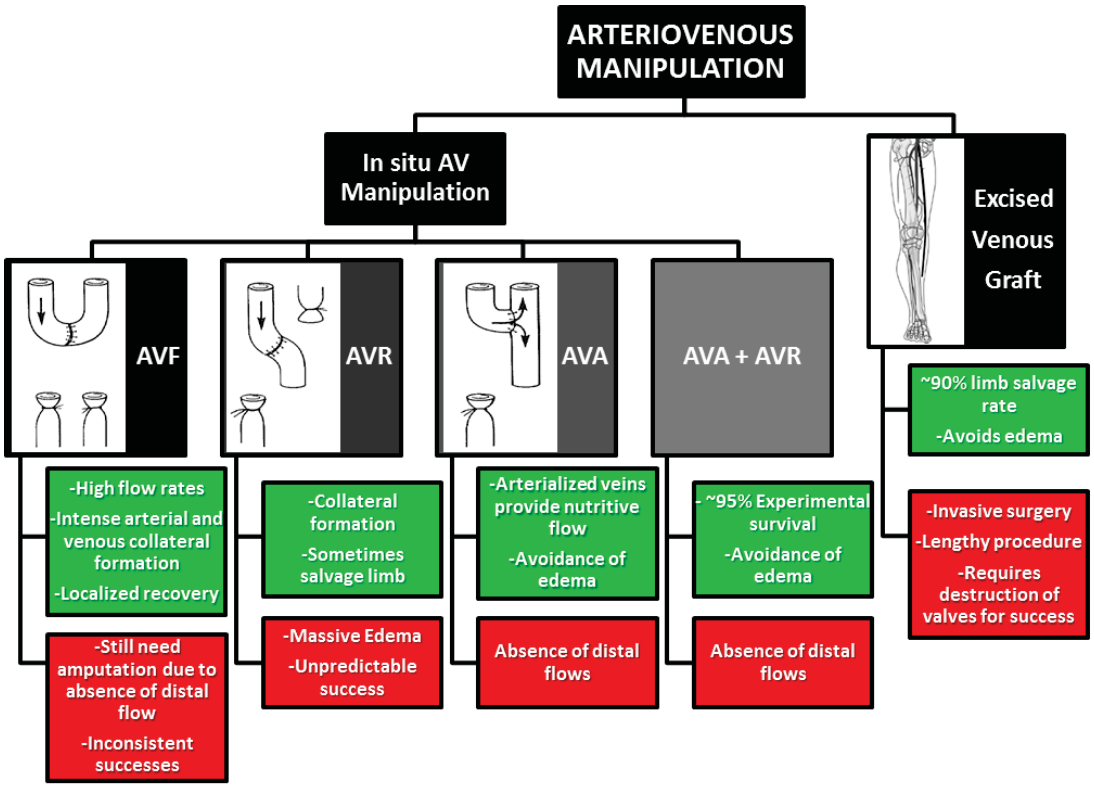

Fig. 1.13. This figure compares the different arterivenous manipulations from in-situ: arteriovenous fistula (AVF), arteriovenous reversal (AVR), arteriovenous anastomosis (AVA), and AVA+AVR, and excised venous graft. (Images from [10, 24]).

salvage investigation. A clinical shift to distal venous arterialization through use of venous excision resulted [33].

1.1.4.2.2. Excised Retroperfusion

Investigators understood the issue with venous valves and their prevention of distal flows, so in order to guarantee the latter, an accessory vein was excised and its valves were destroyed before a distal connection was made in a foot vein (dorsal arch or medial marginal) [33–36]. The recent results are undeniably exciting reaching near

90% success rates of limb salvage [33–36]. Although, the requirements of the success tip the comfort scale as the procedure is highly invasive and lengthy, and destruction of valves are needed before reattachment takes places.

It could be assumed that the ideal retroperfusion technique would avoid edema, avoid valve destruction, avoid an invasive and lengthy surgery all while providing nutritive flow to all ischemic areas and thus salvaging the ischemic limb.

1.2 Objectives

It is believed that all of the current retroperfusion technique concerns can be overcome in a minimally invasive/cather-based approach in which the catheter itself provides a engineered specified resistance that avoids edema and the perfusion location allows for valves to be passable and flow to reach distally. Our approach merges the advantages of both retroperfusion techniques without the repercussions of each of the techniques.

This study is broken up into a series of phases: a theoretical assessment, an ex-vivo proof of concept, an in-vivo validation of the ex-vivo results and gathering of data, and final calculations of an ideal catheter. The theoretical assessment breaks up the study in an engineering approach, which reveals what the unknown parameters are needed for an ideal catheter. The ex-vivo experiments show where and what flows are possible in retroperfusion to indicate what perfusion location to look at in-vivo and what hemodynamics we might expect at that location. The in-vivo experiments address the hemodynamics of the perfusion location under injury, extent of retrograde flow distribution, and metabolic results of injury reversal. The hemodynamic data gathered *invivo* is then added to the theoretical assessment to calculate the ideal catheter resistance needed to obtain a perfusion pressure that will not result in edema.

1.2.1 Hypothesis

We hypothesized that peripheral venous flow reversal can be engineered to a specific pressure-flow range through hemodynamic analysis of retroperfused canine hindlimbs. Evaluation of this hypothesis was pursued through the following objectives.

1.3 Methods

Determine how the catheter resistance relates to the physiological system. By examination of the experimental setup as a catheter in series with the venous vasculature, we could solve for the system variables and manipulate the setup to determine the unknown variables. The unknown variables, venous retro-vasculature and ideal catheter resistance, were then determined through ex-vivo and in-vivo experiments.

Determine the resistance of the venous retro-vasculature most suitable for effective retroperfusion. Because previous retroperfusion efforts have had issues rendering the valves incompetent, we needed to *determine if and where flow reversal was even possible.* Once the valves were shown passable in ex-vivo canine hindlimbs we then circulated fluid to gather pressure and flow rates at various regions of interest in the lower limb to *determine if the retroperfusion hemodynamics were location dependent.* Through capturing location specific hemodynamics, we could then *determine what location would be most suitable for effective retroperfusion* with the characteristics captured at each location.

Determine the resistance of the venous retro-vasculature and characteristics of retroperfusion in-vivo. Because retroperfusion would only take place in an ischemia limb, an ischemia model was needed to gather meaningful retroperfusion data. An extracorporeal circuit was then put into place to *determine the active hemodynamics at the retroperfusion site.* A pressure-flow curve was needed to evaluate the experimental venous retro-vasculature resistance (i.e. the slope of the

curve), the variable needed to calculate an ideal catheter resistance that limits the perfusion pressure to a healthy range. We further characterized the retroperfusion by observing the perfusion territory of the reversed flow. We accomplished this by injecting microspheres in the antegrade arterial route pre-injury and in the reversed venous route post-injury. From here we could get an idea as to where the reversed flow was going, if it was perfusing muscle, which muscles it was perfusing, and overall *how the perfusion territories compared*. Evaluation of distal flow, critical for successful limb salvage, was examined through microspheres in the distal muscles. We also investigated the *metabolic effects of retroperfusion at the chosen perfusion site*, the popliteal vein bifurcation, through blood gas samples. Evaluation of retroperfusion post injury was critical for proof of the perfusion site as a successful location for limb salvage.

Determine the ideal catheter resistance given the hemodynamic data retrieved in in-vivo experiments. The in-vivo experimental pressure-flow data provided us with a value for venous retro-vasculture resistance. Through use of Hemodynamic Ohm's law, we could set our experimental pressure and flows equal to arterial pressure and flows by assuming the same perfusion pressure. A table of ideal catheter resistances given an input/arterial pressure, target perfusion pressures, and arterial flow rates was made for reference for the optimal catheter design of which would be used in clinical setting.

2. OBJECTIVES

We hypothesize that peripheral venous flow reversal can be engineered to a specific pressure-flow range through hemodynamic analysis of retroperfused canine hindlimbs. Evaluation of this hypothesis was pursued through the following specific aims.

2.1 Specific Aims

2.1.1 Specific Aim 1

Determine how the catheter resistance relates to the physiological system. Before any experiments were done an engineering analysis of the system was required to determine what parameters could be manipulated to give the desired output. Because the catheter and the system could be broken down to a series of equations, we hypothesized that the catheter resistance could be engineered to provide a target pressure output range that minimizes edema but still high enough to promote transcapillary exchange.

2.1.2 Specific Aim 2

Determine the resistance of the venous retro-vasculature most suitable for effective retroperfusion. Once the unknown parameter was determined theoretically, a series of experiments were laid out to determine the resistance of the venous retro-vasculature.

2.1.2.1 Specific Aim 2A

Determine whether flow reversals are possible. Because previous retroperfusion efforts had issues rendering the valves incompetent, we needed to explore if and where flow reversal was even possible. Because a series of in-situ flow reversals were shown to be possible [29,30] and not [19], we hypothesized that the valves were passable but would be location dependent.

2.1.2.2 Specific Aim 2B

Determine if the retroperfusion hemodynamics is location dependent. Because the incompentency of valves were assumed to be location dependent we also assumed the retroperfusion hemodynamic characteristics to be location dependent as well. This means that the resistance of the venous retro-vasculature was hypothesized to be different depending on the location of perfusion.

2.1.2.3 Specific Aim 2C

Determine what location would be most suitable for effective retroperfusion. After observing retroperfusion at various locations, one site was decided as the most promising for effective retroperfusion and would be used for in-vivo analysis. Because the venous system is very interconnected to allow for flow to travel the path of least resistance, we hypothesized that very distal locations would succumb to venous-venous shunting whereas more proximal locations can avoid this mostly by being out of venous-venous collateral network.

2.1.3 Specific Aim 3

Determine the resistance of the venous retro-vasculature and characteristics of retroperfusion in-vivo. Once a retroperfusion location was decided from ex-vivo experiments, the same location was explored in-vivo for further analysis.

2.1.3.1 Specific Aim 3A

Determine the active hemodynamics at the retroperfusion site. The pressure-flow relation was collected in-vivo to determine a more realistic relationship between pressure and flow. Because the venous system has limited control of flow regulation we hypothesized the hemodynamic characteristics to be similar to ex-vivo.

2.1.3.2 Specific Aim 3B

Determine the perfusion territory of venous reversed flow compared to arterial forward flow. The forward and reversed flow was analyzed to determine if any of reversed flow reached the ischemic muscle. Because previous studies had success with retroperfusion at the same perfusion site [29,30], we expected to observe some of the reversed flow in the ischemic muscles.

2.1.3.3 Specific Aim 3C

Determine the effects of retroperfusion on an acute hindlimb ischemia canine model. To validate the potential of the retroperfusion site as a beneficial location to start reversed flow, we analyzed the metabolic effects of retroperfusion throughout the experiment. Because previous studies had shown success with retroperfusion at the same perfusion site [29,30], we expected some change in metabolites due to retroperfusion.

2.1.4 Specific Aim 4

Determine the ideal catheter resistance given the hemodynamic data retrieved in in-vivo experiments. By taking the hemodynamic data collected in-vivo, we could then back calculate to find the ideal catheter resistance that would result in target output pressures given the work done in Aim 1.

Ultimately work would be done by theoretically assessing peripheral venous retroperfusion and experimentally collecting the characteristics and evidence of retroperfusion as a potentially engineerable therapeutic option for patients with critical limb ischemia.

3. METHODS

3.1 Theoretical Basis

Characterization of the catheter and physiological system was done through a circuit design using fundamental hemodynamic properties.

Determine how the catheter resistance relates to the physiological system.

Mathematically, the catheter was assumed to be in series with the venous vasculature. Because blood flow is characterized similar to electricity we thought of the setup as circuit, but instead of Ohm's Law ($V = IR$) we used Equation 3.1 [1]. From here, basic laws of hemodynamics were used to further evaluate the retroperfusion system. The components and parameters of the system are shown in Figure 3.1.

$$\Delta P = QR, \tag{3.1}$$

The input source ($Pressure_{Input}$) to the system, clinically, would be the arterial pressure ($IP_{Catheter}$) and flow at the proximal end of the catheter located inside the artery, the catheter resistance itself ($R_{Catheter}$), the catheter output pressure ($OP_{Catheter}$) or perfusion pressure ($IP_{Vasculature}$) inside the vein, the venous vasculature resistance ($R_{Vasculature}$), and the pressure once the flow has left the venous system ($OP_{Vasculature}$).

Fundamental hemodynamic Equation (3.1) was then used to solve for various parameters.

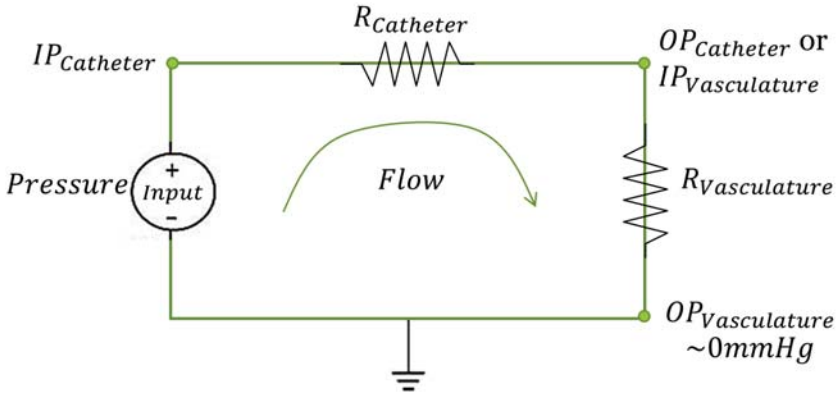

Fig. 3.1. This figure shows the theoretical circuit of the experimental setup and logic to solving unknown variables.

3.2 Ex-vivo Experiments

Ex-vivo hindlimbs were immediately amputated from a healthy acute canine. The femoral artery was exposed and a 4F sheath was sutured in place. 10ml of heparin was mixed into a 1l saline bag. A flushed IV line was added to the cannula and the drip rate was adjusted to 1 drip/second. Once the heparinized saline finished flushing the lower vasculature through the arterial system, the cannula was closed off. A radiopaque hydrophillic guidewire was then advanced through the femoral vein under fluoroscopy.

Once the valves were confirmed to be passable, the passive hemodynamics of three locations were explored. The guidewire was first advanced to the location of interest and then a flushed catheter replaced the wire. To prevent immediate backflow the tip of the catheter was either ligated or a balloon was inflated. The catheter was attached to an experimental setup of pulsatile, retrograde flow. Various pressure inputs and outputs to the catheter and flow rates were recorded to capture the passive hemodynamics of the system.

Determine whether flow reversals are possible.

Valve Experimentation. After the lower vasculature was flushed with heparinized saline, a wet hydrophillic guidewire (Roadrunner; Cook Medical, Bloomington, IN) was advanced barebacked through the femoral vein under fluoroscopy. To pass the proximal valves either some moderate forward flow was connected to the arterial cannula and/or the wire was pulled backed and pushed forward until the valve was passed. The wire was kept very wet and sometimes the leg was straightened to pass difficult turns in the venous system.

Determine if the retroperfusion hemodynamics is location dependent.

Locations of Interest. Once the valves were passed, three locations had their passive hemodynamics captured. The locations explored were referred to as 'distal', 'midway', and 'proximal' located at the venous dorsum pedis, the lateral saphenous vein bifucation, and the popliteal vein bifurication, respectively. Each of the locations explored in ex-vivo are shown in Figure 3.2 with respect to the ex-vivo leg with tissue intact, fluoroscopy, and ex-vivo leg after cut down.

Retroperfusion Preparation. The hydrophilic guidewire was advanced to the distal location and then a flushed catheter was advanced over the wire. Confirmation of the location of interest was confirmed under fluoroscopy. Before any retro flow was added to the system an experimental setup to capture all the circuit parameters of pressure and flow were put into place.

Experimental Setup. The experimental setup consisted of a fluid transducer, a pressure wire (ComboWire XT Guide Wire; Volcano Corp, Alpharetta, GA), a flow probe and flowmeter (Transonic Systems Inc, Ithaca, NY), a data acquisition system (Biopac, Goleta, CA), and a computer to collect the inlet pressure to the catheter, the outlet pressure to the catheter, the flow rate into the catheter, the data from the fluid transducer and the flow meter and the DAQ data, respectively and a flow pump to supply the system with a pulsatile flow. Figure 3.3 shows where each of the parameters were detected.

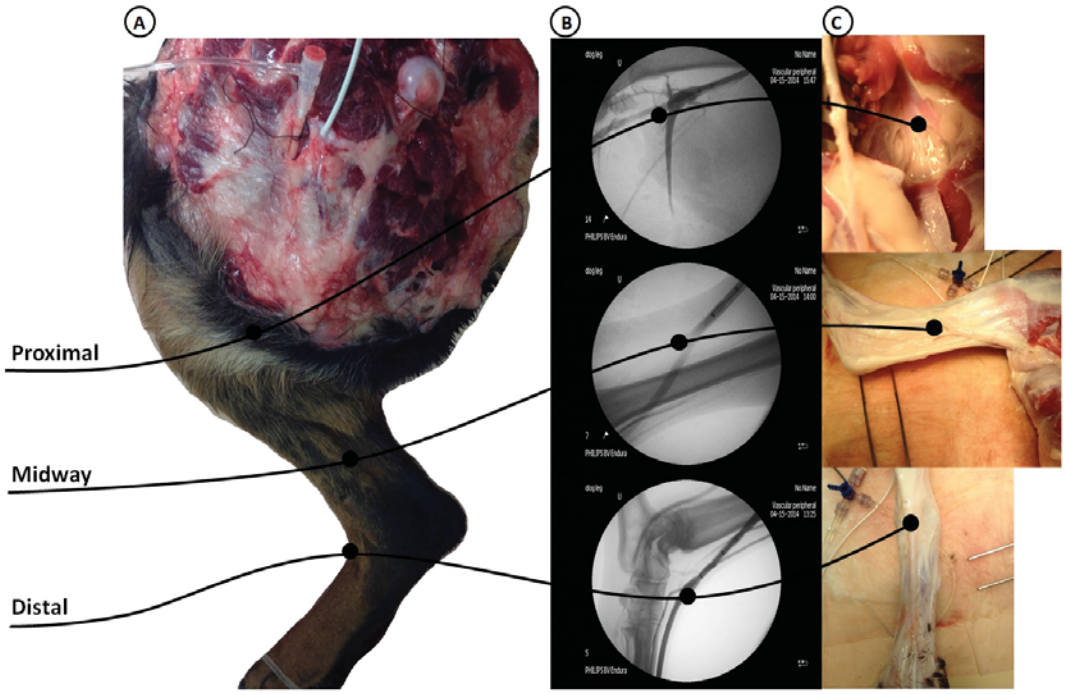

Fig. 3.2. This figure shows the locations explored during the ex-vivo experiments with respect to (A) the ex-vivo leg with tissue intact (medial view), (B) fluoroscopy (medial view), and (C) ex-vivo leg after cut down (medial, lateral, and plantar view, respectively), where distal is the venous dorsum pedis, midway is the lateral saphenous vein bifurcation, and proximal is the popliteal vein bifurcation.

Parameters. Experimentally, $Pressure_{Input}$ was the inlet source of the flow pump, which pulled from a solution of 6% dextran. The inlet pressure of the catheter ($IP_{Catheter}$) was detected from a flushed pressure line hooked up to a calibrated fluid transducer. A 5mm flow probe then sensed the flow rate through a calibration material. The pressure wire was placed in catheter to the location of constant flow and normalized from the command station then advanced to the tip of catheter to collect the outlet pressure of the catheter ($OP_{Catheter}$). Once in place, the port was screwed closed and either a balloon was inflated, or the tip of the catheter was ligated to prevent immediate back flow. (Figure 3.3 shows a balloon inflation port).

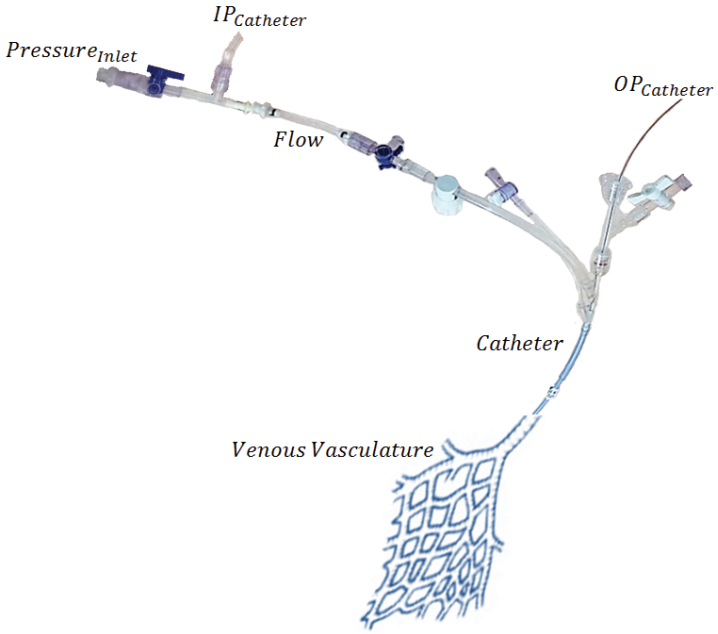

Fig. 3.3. This figure shows where each of the system parameters are being detected from the experimental setup.

Retroperfusion Measurements. The flushed tubing from the flow pump was connected to the catheter setup, and once no bubbles were confirmed in the line the pump was turned on the lowest flow rate and stepped up by increments enough to capture at least every 10mmHg, with approximately 30-45 seconds at each pressure, and shut off once pressures begin to plateau or reach 100 mmHg.

Once done at the distal location, the inflation or ligature was removed and either the pressure wire was kept distal to confirm pressures when perfusing from a higher location or the entire system was pulled back to the next location.

Analysis. All pressures and flow data were collected in AcqKnowledge. The data was averaged over a homeostatic segment that consisted of 3-5 waveforms.

3.3 In-vivo Experiments

Animal Preparation. Following overnight fasting, 6 mongrel dogs with 10 weeks of venous hypertension were sedated with acepromazine (0.025-0.1 mg/kg) and butorphanol (0.2-0.4 mg/kg) either intramuscular or subcutaneous 30 minutes prior to final induction of isofluorane, quickly intubated, and further anethesized with isofluorane (2%) and 100% oxygen. An IV line was introduced in their cephalic vein for continuous infusion of saline with a drip rate of 20 drips/minute. They were placed on a circulating hot water pad, and their neck, lower abdomen/iliac, and popliteal levels were shaved. A pulse oximeter was placed on their tongue, a blood pressure cuff on their right brachealcephalis, and a thermometer in the back of the throat, for vital recordings of heart rate/oxygen saturation, blood pressure, and temperature, respectively.

Both carotid arteries were accessed with a 9F sheath to supply nutritive blood to the extracorporeal circuit and to have a catheter (Catheter A) at the popliteal artery to collect the retroperfusion effluent after an angiogram of popliteal arterial system was performed. One jugular vein was accessed with a 8F sheath to infuse 3000 units of heparin every 1-2 hours.

Baseline Measurements. Initial baseline velocity measurements were made from ultrasound doppler PW at the popliteal artery and vein bifurcation. The pulse oximeter was placed between their toes and on their superficial digital flexor to detect spO2. Central blood samples were taken and an arteriogram of the popliteal network was perform with a White Lumax Catheter, Catheter A. Microspheres were then injected at the popliteal artery bifurcation before the injury took place.

Injury Model. An ischemic hind-limb was prepared in the either the left or right hind-limb of all the animals by arterial ligation at the descending aortic bifurcation, both external iliac arteries, and the terminal aorta (Figure 3.4). Occlusion was confirmed by contrast injection of Catheter A. After approximately 1 hour of occlusion and at 2-3 hours of occlusion, blood samples were taken (Cook Medical, Bloomington, IN).

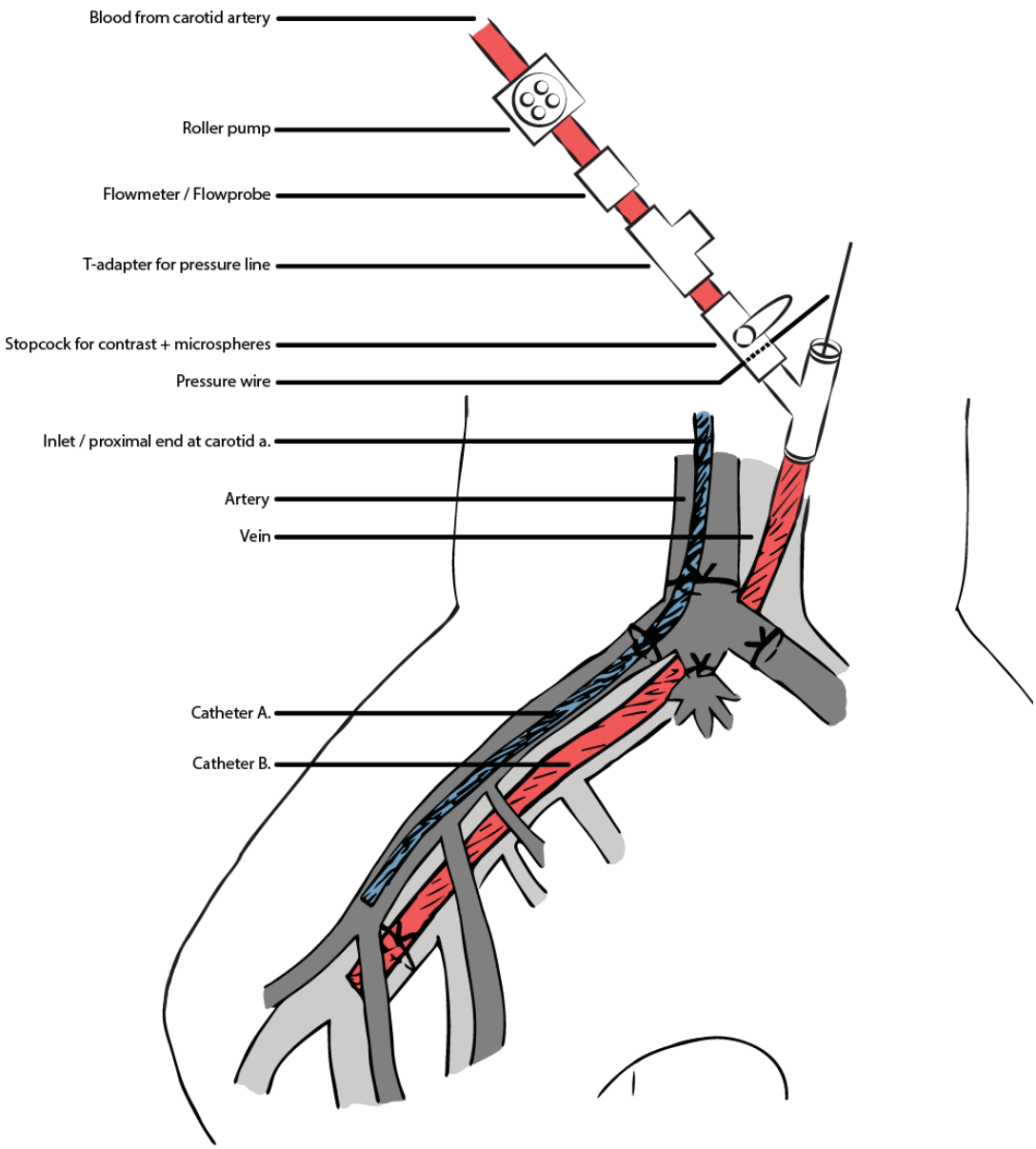

Fig. 3.4. This figure shows where each of the injury ligations are located, the system parameters are being detected, and the catheter locations. Catheter A was left in the arterial system for effluent retrieval and Catheter B was the retroperfusion catheter.

Retroperfusion Preparation. Re-perfusion of the microsphered leg began by cannulation of the common iliac vein with a 9F sheath. Under fluoroscopy, a radiopaque hydrophilic guidewire was advanced to the popliteal vein bifurcation and then another flushed white lumax catheter, Catheter B, replaced the wire. The tip of the catheter was ligated and once no back flow was confirmed under fluoroscopy Catheter B was connected to the extracorporeal circuit and flow was added to the circuit.

Final Measurements. The pressure wire was first normalized and put into place, then the catheter was flushed with blood being pulled from the central carotid artery line. Microspheres were injected at the popliteal vein birucation from Catheter B. The circuit was reattached to Catheter B and retroperfusion began. After all the necessary pressure flow was collected, blood samples were collected and the pump was shut off. The animal was sacrificed with a saturated bolus of potassium chloride, and muscle samples were immediately taken from the experimental leg.

Determine the resistance of the venous retro-vasculature and characteristics of retroperfusion in-vivo.

Extracorporeal Circuit. The extracorporeal circuit, similar to the ex-vivo experimental setup, consisted of a fluid transducer, a Volcano Combo wire, a flowmeter, a data acquisition system (Biopac), and a computer to collect the inlet pressure to catheter b, the outlet pressure to catheter b, the flow rate into catheter b, the data from the fluid transducer and the flow meter, and the DAQ data, respectively and a flow pump to supply the system with a pulsatile flow. Figure 3.5 shows where each of the parameters are detected.

Parameters. Acutely, $Pressure_{Input}$ was the supply source of the flow pump, which pulled from the central carotid artery line. The inlet pressure of the catheter ($IP_{Catheter}$) was detected from a flushed pressure line hooked up to a calibrated fluid transducer. A 5mm flow probe then sensed the flow rate through a calibration material. The pressure wire was placed in catheter b to the location of constant flow and normalized from the command station then advanced to the tip of catheter to collect

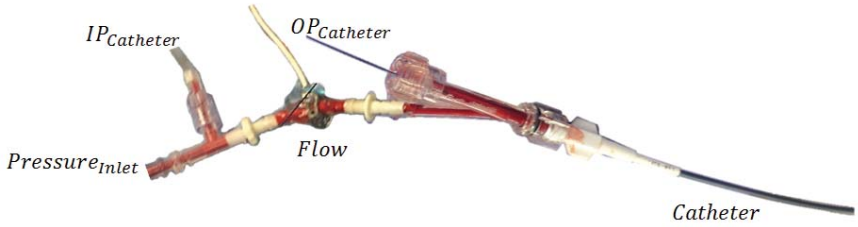

Fig. 3.5. This figure shows where each of the system parameters are being detected from the experimental setup.

the outlet pressure of the catheter ($OP_{Catheter}$). Once in place, the port was screwed closed and the tip of the catheter was ligated to prevent immediate back flow.

Retroperfusion. After microsphere flushing, the stop cock was replaced, the line was filled with fresh blood, and the circuit was reattached to catheter b as the pump starting retroperfusing at the lowest flow rate. Approximately 1-3 minutes of perfusion was performed at each flow rate or until steady-state pressures resulted, then the flow rate was stepped up by increments enough to capture at least every 10 mmHg and stopped increasing the flow rate once distal pressures ($OP_{Catheter}$) begin to reach between 70-80 mmHg. Retroperfusion was performed for approximately one hour per animal.

Analysis. All pressures and flow data were collected in AcqKnowledge. The data was averaged over a homeostatic segment that consisted of 3-5 waveforms.

Determine the perfusion territory of venous reversed flow compared to arterial forward flow.

Baseline. Before the injury-occlusion took place, 15μm blue fluorescent microspheres (FluoSpheres Blood Flow; Life Technologies Corporation, Carlsbad, CA) were injected at the popliteal artery bifurcation by mixing 1.62 ml of microspheres with manually mixed in with 15 ml of nutritive blood in a 20 ml syringe by use of a stopcock. After mixing at a rate of 1 ml/sec for two-three minutes, 1 ml of microsphere

mixed blood was injected into catheter a every 10 seconds, with one to two mixes inbetween each injection. Once all the microspheres were injected the syringes were flushed with 10-15 ml of saline using the same mixing and injection technique.

Retroperfusion. Catheter b was flushed before microsphere injections. The arterial blood filled tubing from the flow pump was connected to the catheter setup, and once no bubbles were confirmed in the line the pump was turned on the lowest setting for approximately one minute to flush catheter b with nutritive blood. The pump was turned off and detached from catheter b and a stopcock was placed at the inlet port in which 0.62 ml of yellow-green microspheres were mixed with 10 ml of blood and injected using the same mixing, injecting, and flushing method as baseline microspheres.

Analysis. Muscle from the experimental leg was immediately excised in 1-3 gram segments in 15 ml conicals for microsphere analysis after the animals were sacrificed. The muscle digestion, filtration, microsphere digestion, and fluorescence measurements were made according to the Fluorescent Microspheres Resource Center [41] and to the Molecular Probe's Product Information of the FluoSpheres [42].

The sample locations and weights were recorded. Locations of interest starting from closest muscle to the perfusion site is the lateral long digital extensor, to anterior cranial tibial, to posterior medial head to lateral head, next to lateral midway at superficial digital flexor, to its distal segment to the deep muscle fibularis brevis, to top of foot (extensor digitalis brevis) to bottom of foot (interosseous) (Figure 3.7).

Potassium hydroxide (4M) was added to each sample at a volume of approximately 4-5 times the sample's weight (per gram). The muscle samples were kept in the dark and at room temperature for two weeks for adequate tissue digestion.

The fat was removed from the top layer of the digested muscle by pipette suction. The sides of the conical were cleaned with a KimWipe and once all possible fat deposits were removed the conical was vortexed to homogenize the hydrolysate containing the digested tissue and microspheres. The digested tissue and microsphere were then physically separated using a negative pressure filtration system (Figure 3.6).

The outer shell of the Perkin Elmer Filtration Unit was placed inside an Erlenmeyer flask. To make a tight seal, 4mm plastic tubing was wrapped around the outershell and parafilmed to the flask. In Step 1 the sample tube (Poretic polycarbonate 8μm filters) was placed inside the outshell and the homogenized hydrolysate was poured over the filtered sample tube. The conical then had 4M KOH added (half the original hydrolysate volume), vortexed, and poured over the filter to collect the remaining microspheres in the conicals. This process was repeated three times to ensure all remaining microspheres were collected. In Step 2 the filter was carefully removed from the tube (clean forceps were used to dislodge the filter from the tube from the underside). In Step 3 the filter was placed in a clean fluorescent 10mm pathlength cuvette (3.5ml Glass Cell G214; Fisher Scientific, Hanover Park, IL). Cellosolve acetate (2 ml) was added to the cuvette, closed with its stopper, and placed in the dark as the microspheres digested for 1 hour.

After the hour of microsphere digestion, the cuvette had its fluorescence read from a spectrometer (Spectramax M2e; Molecular Devices, Sunnyvale, CA) by exciting the dyes at their specific wavelengths and recording the emission light at their respective maximum emission wavelengths specific to Cellosolve acetate (Blue (356,424), Yellow-Green (495,505)). Every sample was excited and recorded 2-3 times to ensure consistent fluorescent values. Their fluorescence intensities were made relative to each other according to the Fluorescent Microspheres Resource Center Standard Curves and to their injected volumes.

A new filtered sample tube was used for each sample, and the forceps, cuvette, and stopper were thoroughly cleaned with methanol between each sample.

Determine the effects of retroperfusion on an acute hindlimb ischemia canine model.

All blood samples were collected in a 3ml heparinized syringe, immediately closed with a capped 22 gauge needle to maintain in-vivo metabolite levels, and placed on ice.

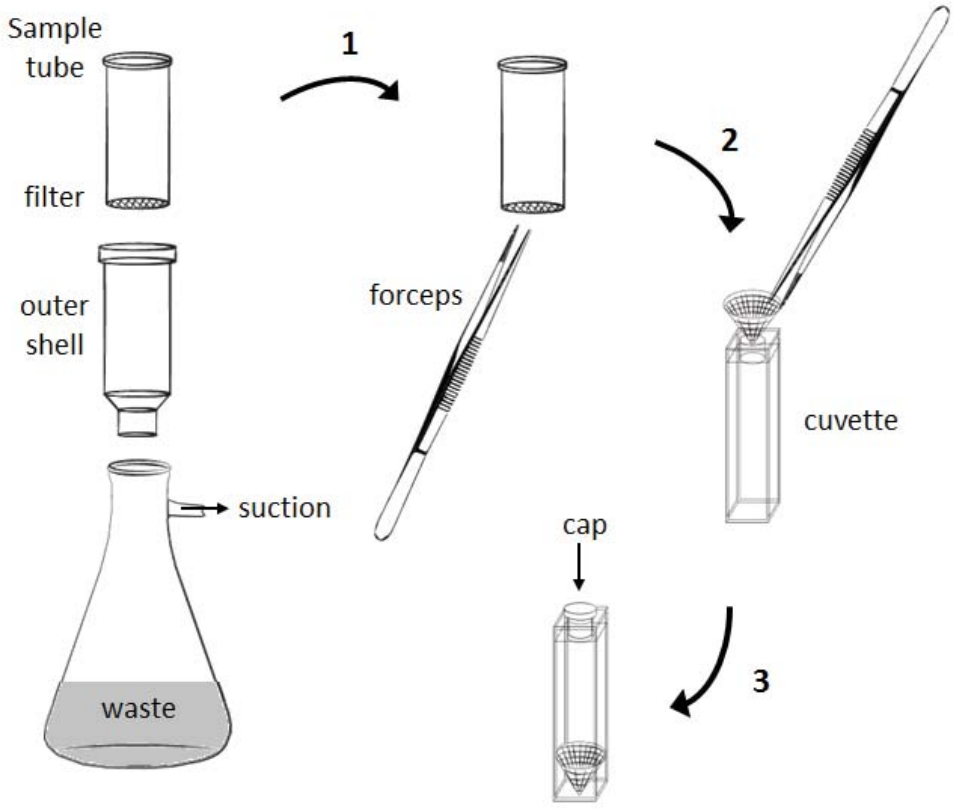

Fig. 3.6. This figure shows the negative pressure filtration system used for filtrating the microspheres.

Baseline. Central blood samples were taken from the carotid artery and jugular vein before microspheres were injected.

Occlusion. After approximately 1 hour of occlusion, blood samples were taken from the catheter a to collect the occlusion effluent, and from the central arterial and venous sheaths. Blood samples were again collected at 2-3 hours of occlusion and placed on ice.

Retroperfusion. After the pressure and flow retroperfusio data was collected, blood samples were taken from catheter a to collect the occlusion effluent, and from the central arterial and venous sheaths.

Analysis. All blood samples were analyzed within 3 hours of collection using a blood gas analyzer (GEM Premier 3000; Instrumentation Laboratory Company, Bedford, MA) and a CO-oximeter (682) system (Instrumentation Laboratory Company).

3.4 Theoretical Assessment

Determine the ideal catheter resistance given the hemodynamic data retrieved in in-vivo experiments. The ideal catheter resistance was calculated by assuming the outlet pressure received in-vivo would be the same for the actual clinical setting of the implanted catheter. By use of Equation 3.1 again, a series of manipulations were done to solve for the unknown variable, ideal catheter resistance.

$$\Delta P = P_{In} - P_{Out} = QR,$$

$$P_{Out} = P_{In} - QR,$$

$$OP_{Catheter} = IP_{Catheter} - QR,$$

$$OP_{Catheter_{Experimental}} = OP_{Catheter_{Actual}},$$

$$IP_{Catheter_E} - Q_E R_{Catheter_E} = IP_{Catheter_A} - Q_A R_{Catheter_A},$$

$$R_{Catheter_A} = \frac{IP_{Catheter_A} - IP_{Catheter_E} + Q_E R_{Catheter_E}}{Q_A} \tag{3.2}$$

Where $R_{Catheter_A}$ is the theoretical ideal catheter resistance, $IP_{Catheter_A}$ is typical arterial pressures at the proximal end of the catheter, $IP_{Catheter_E}$ was the inlet pressures detected at the proximal end of the experimental catheter of the grouped in-vivo data, Q_E was the respective flow rates of the grouped in-vivo data, $R_{Catheter_E}$ was the averaged experimental slopes of the ΔP and flow curves of each animal, and Q_A is typical arterial flow rates the implanted catheter might experience.

3.5 Statistical Analysis

All data was presented as mean ± standard error. Analysis of Covariance was used to detect statistical differences between slope and y-intercept in linear fitted results using the statistical software GraphPad Prism 5 with p values $p < .05$, $p < 0.01$, $p < 0.001$, and $p < .0001$, represented as *, **, ***, and ****, respectively. 2-sample t-test was used to detect statistical differences between mean data (blood gas results) in Minitab 17 with p values $p < .05$, $p < 0.01$, and $p < 0.001$ represented as *, **, and ***, respectively.

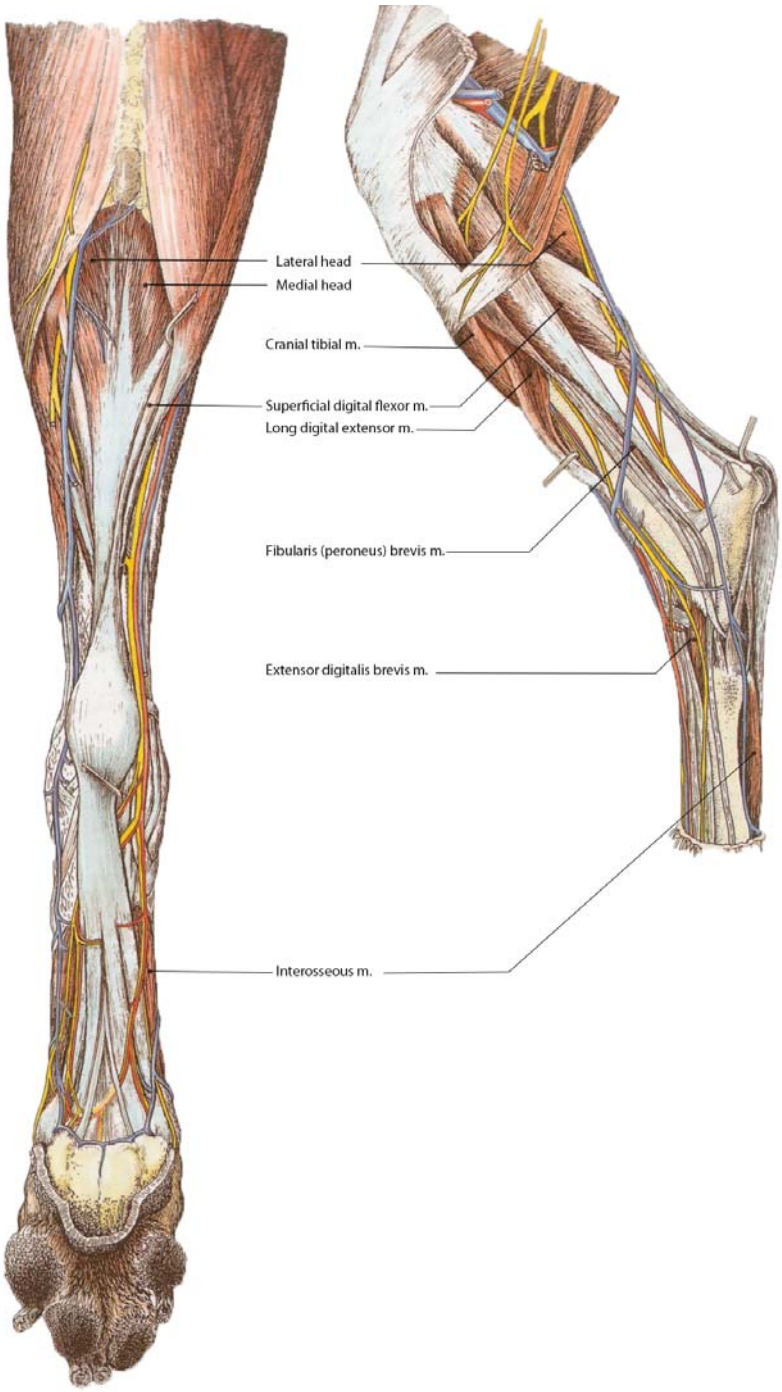

Fig. 3.7. This figure shows the different muscles of interest for the microsphere analysis of forward perfusion and retrograde perfusion [43].

4. RESULTS

4.1 Theoretical Basis

Determine how the catheter resistance relates to the physiological system.

By examining the experimental setup as a circuit, mathematical manipulations were made to the setup to determine what variables of the system were known and unknown. Through evaluation of the parameters displayed in Figure 3.1, the known and unknown parameters are shown in Table 4.1.

The unknown variables, venous retro-vasculature and ideal catheter resistance, were then determined through ex-vivo and in-vivo experiments.

4.2 Ex-vivo Experiments

Determine whether flow reversals are possible.

In order to characterize the retro venous vasculature ex-vivo canine limbs were investigated for practicality. First the venous valves were experimentally explored for the best method of advancement to reach the distal limb. Figure 4.1 shows the radiopaque hydrophillic guidewire advanced retrogradely through the venous system all the way down into the dog's foot under fluoroscopy.

Determine if the retroperfusion hemodynamics is location dependent.

After the valves were experimentally determined to be passable, three distal venous locations were further explored. Figure 4.2 shows (A) the 'proximal' location (popliteal venous bifurcation), (B) the 'midway' location (lateral saphenous vein bifurcation), and (C) the 'distal' location (dorsum pedis vein) under fluorscopy. Both

Table 4.1.
Known and Unknown Parameters of Theoretical Circuit

Parameter	Condition	Clinical Location	Clinical Specification
$Pressure_{Input}$	Known	Most Distal Satisfactory Artery	Arterial Inputs
$IP_{Catheter}$	Known	Proximal End of Catheter Inside Artery	Mean Pressure of ∼100mmHg
$Flow$	Known	Proximal End of Catheter Inside Artery	Flow Rate of ∼300ml/min
$R_{Catheter}$	Unknown	Proximal End in Artery and Distal End in Vein	Experimentally Determined
$OP_{Catheter}$ or $IP_{Vasculature}$	Known	Distal End of Catheter Inside Vein	Target between 40-60mmHg
$R_{Vasculature}$	Unknown	Retro Venous Vasculature	Experimentally Determined
$OP_{Vasculature}$	Known	Distal End of Vasculature	Assumed to be 0mmHg

proximal images show the extensive venous network at the popliteal bifurcation with the right image displaying tortosity in the cranial tibial vein. The left midway image shows an immediate shunt occurring in the medial saphenous vein and the right shows the lateral saphenous vein with the same tortuous characteristic seen in the cranial tibial vein. Both distal images display the various shunts when the flow is far in the foot.

After a venogram was made at each of the ex-vivo locations, the passive hemodynamic characteristics were captured. An experimental setup that collected the pressures at both end of the perfusing catheter and the flow rate was put into place after no backflow at the catheter was confirmed. Graph A in Figure 4.3 shows the

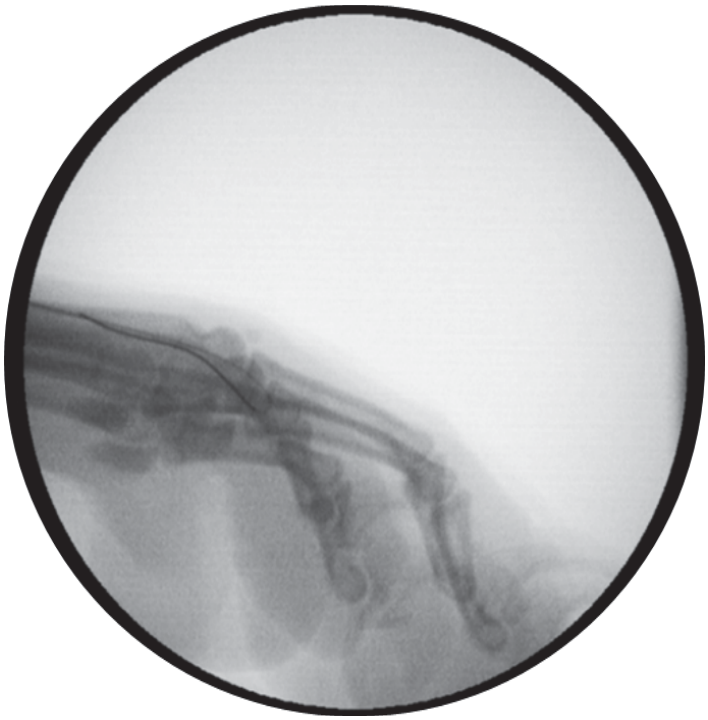

Fig. 4.1. This figure shows the guidewire down in the ex-vivo dog's foot thus surpassing all proximal venous valves.

raw data at each of the locations in which the data is fairly jumbled together in a linear fashion. Graph B confirms the linearity of the data once the data is cleaned up into bins of 5ml/min (e.g. $(0, 5]$) with the average flow rate and pressure shown and their respective standard error.

To test whether the hemodynamics at each location was different, Analysis of Covariance (ANCOVA) was performed to the test the statistical difference of the slopes and y-intercepts. Graph A in Figure 4.4 shows each location's linearized equation and r-squared value. No slope was statistically different, but the proximal and midway's y-intercept was significantly different from the distal location, $p < 0.001$ and $p < 0.01$, respectively. Because the proximal and midway's slope and y-intercept were not statistically different, their data was combined into one location, proximal.

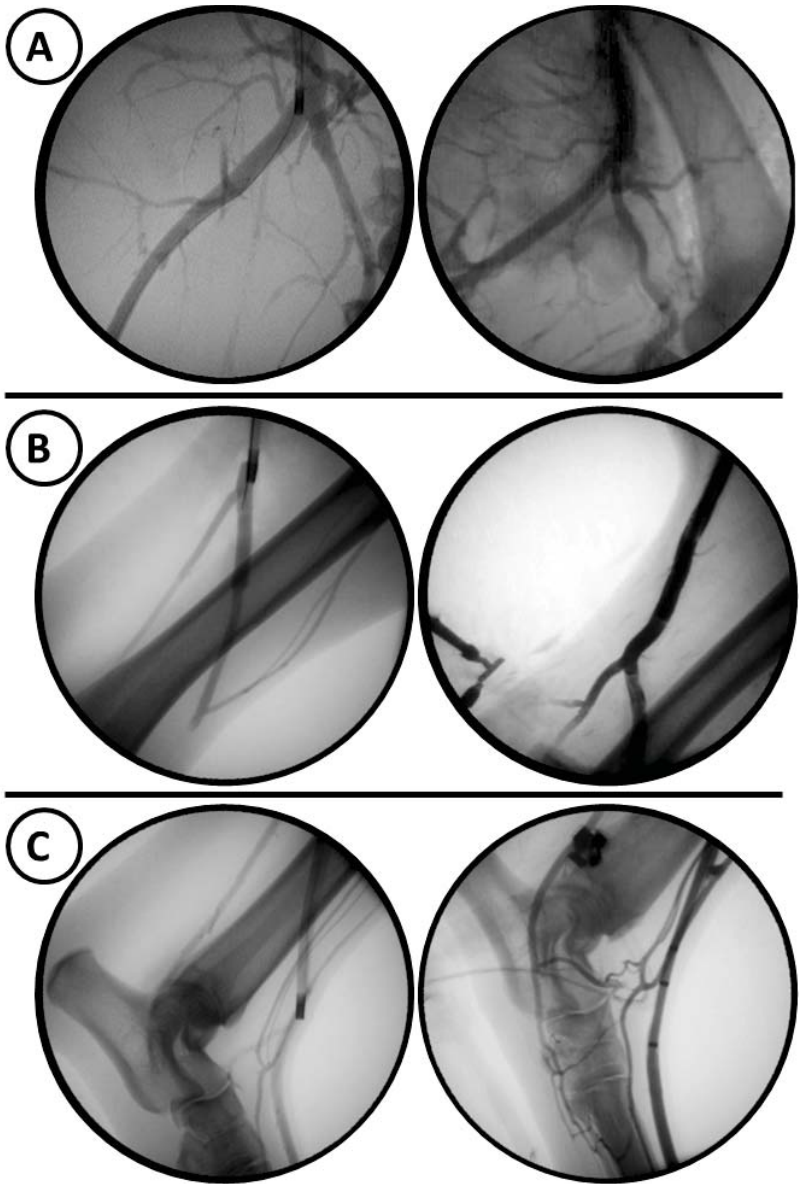

Fig. 4.2. This figure shows the ex-vivo locations under fluoroscopy. (A) is the proximal or popliteal venous bifurcation, (B) is the midway or lateral saphenous vein bifurcation, and (C) is the distal or dorsum pedis vein.

Graph B in Figure 4.4 shows the combined proximal data to the distal location, in which the y-intercept is still statistically different, $p < 0.01$.

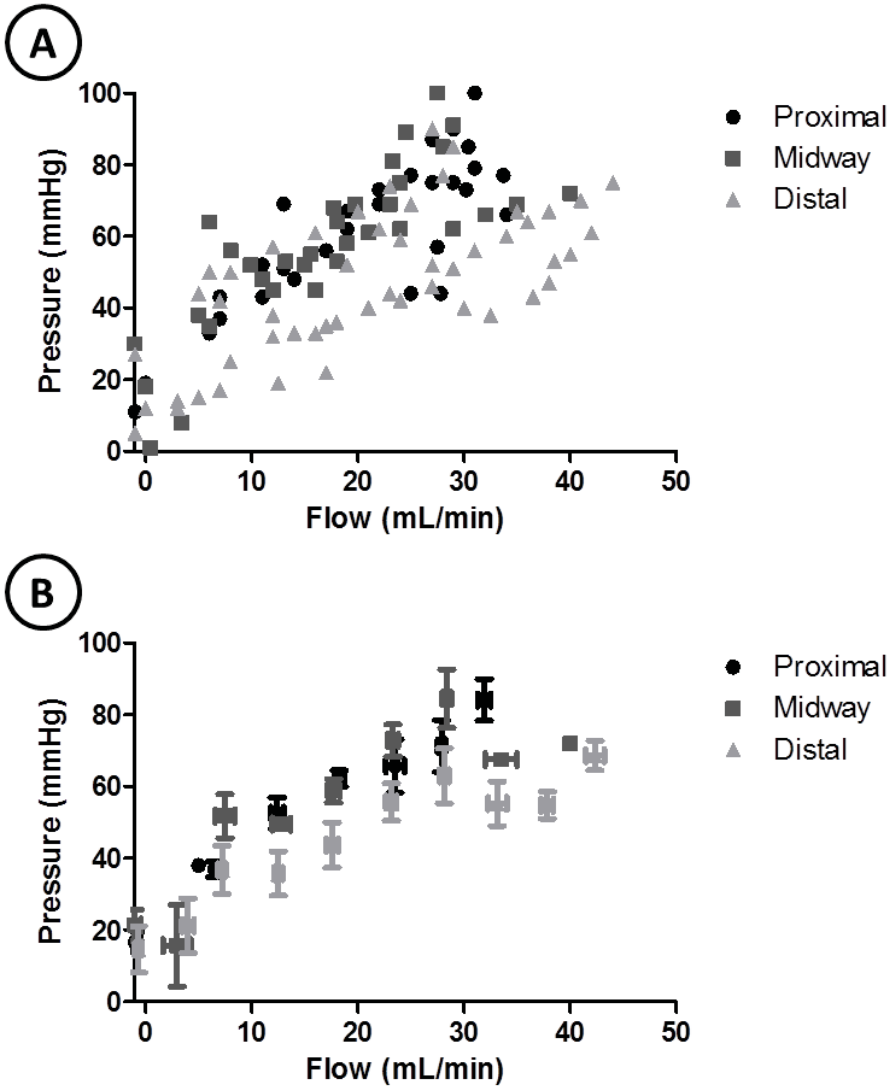

Fig. 4.3. This figure shows (A) the raw pressure flow data at each of the perfused sites and (B) the data put into bins of 5ml/min.

The hemodynamics at the popliteal vein bifurcation was explored in-vivo in an active state.

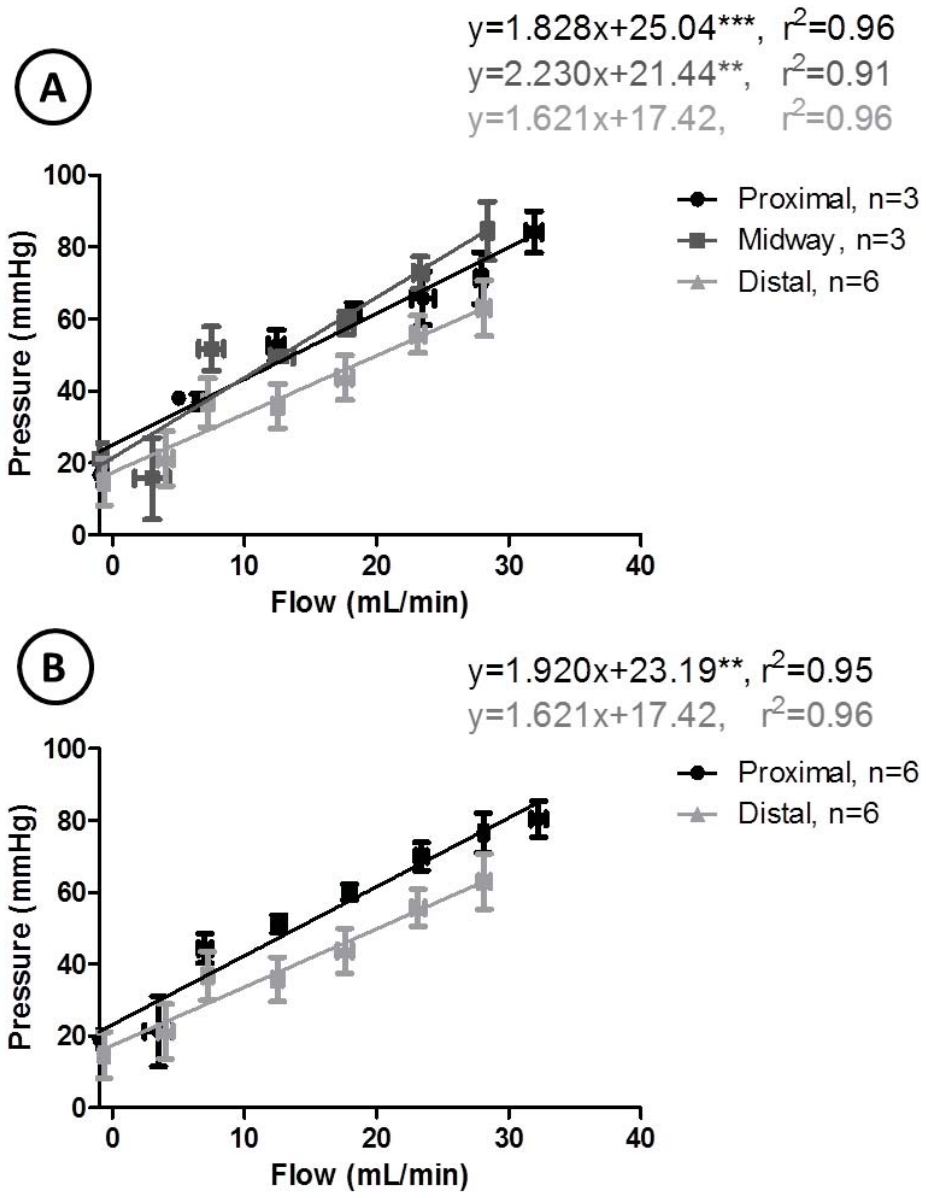

Fig. 4.4. This figure shows (A) the linearized data from each of the locations and (B) the proximal and midway data combined for new proximal data. ** represents statistical significance of $p < 0.01$ and *** of $p < 0.001$ vs each location's y-intercept.

4.3 In-vivo Experiments

Determine the active hemodynamics at the retroperfusion site.

After an acute hindlimb injury was made, the active hemodynamic characteristics were captured. An experimental setup that collected the pressures at boths end of the perfusing catheter and the flow rate was put into place after no backflow at the catheter was confirmed. Graph A in Figure 4.5 shows the raw data for each animal. The data appears to be fairly linear and together. Graph B lumps the data into bins of 5ml/min and is compared to the ex-vivo combined proximal data.

To further investigate the differences of the passive and active hemodynamics at the popliteal vein bifurcation, the linearized portion of the data was fit to a linear regression and their slopes and y-intercepts were compared using an ANCOVA test. The slopes were not statistically different but the y-intercepts were ($p < 0.0001$).

Determine the perfusion territory of venous reversed flow compared to arterial forward flow.

To test where the reversed flow went in-vivo, analysis of forward flow at the popliteal artery bifurcation (baseline) and reversed flow at the popliteal vein bifurcation (retroperfusion) were compared using different colored microspheres. Image A in Figure 4.7 show an arteriogram at the popliteal artery bifurcation. Image B shows an arteriogram after the initial contrast injection and reveals the contrast leaving the leg through the lateral saphenous vein. A venogram at the popliteal vein bifurcation is displayed in image C and D where image D shows both experimental catheters in place.

Once the arteriogram and venogram were made to confirm to the location, microspheres were injected. At the end of the experiment, muscle samples were taken from various locations throughout the experimental distal limb. The muscle samples were digested and microspheres were filtered from the digestion using a negative pressure filtration system. The filtered micrspheres were then digested to allow their respective fluorescence to escape. The fluorescence of each microsphere injection was

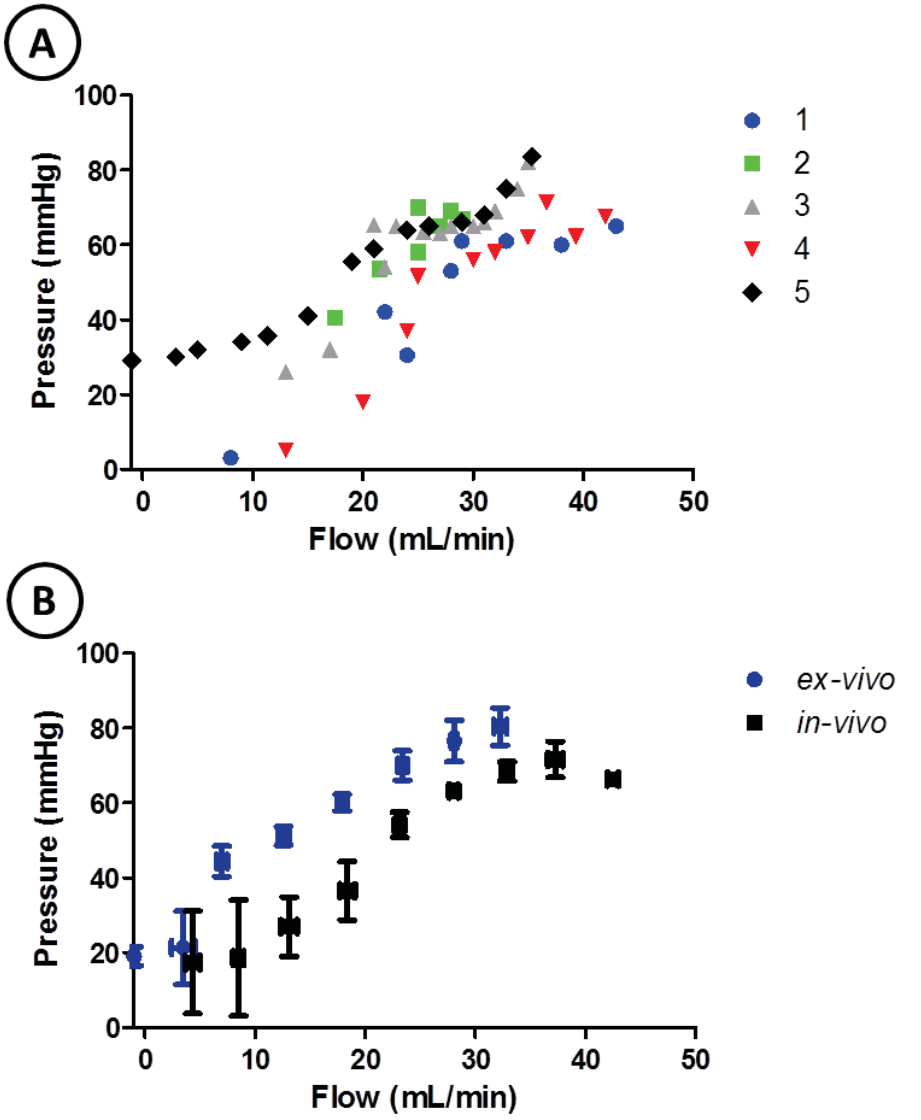

Fig. 4.5. This figure shows the raw in-vivo pressure flow data (A) for each animal and (B) the data lumped into bins of 5ml/min and compared to the ex-vivo combined proximal data at the popliteal vein bifurcation.

detected, blue for baseline and yellow-green for retroperfusion. Graph A in Figure 4.8 shows the relative fluorescence intensity per gram tissue of the forward perfusion territory (baseline) and retrograde perfusion territory (retroperfusion). The relative

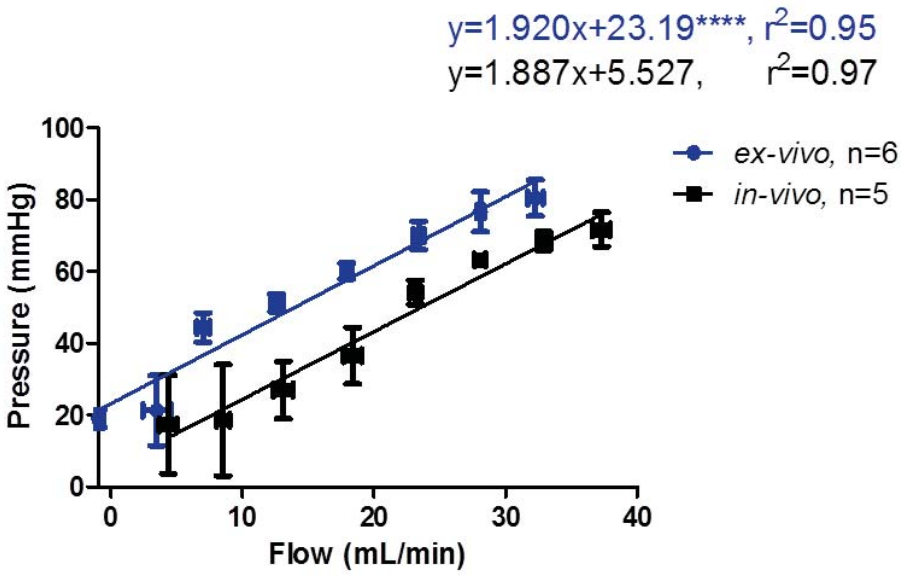

Fig. 4.6. This figure shows the characteristics of the ex-vivo data at the combined proximal location and in-vivo data at the popliteal vein bifurcation. **** indicates $p < 0.0001$ vs each experimental y-intercept.

levels of the retroperfused fluorescence trends similarly to the respective location with a slight increase in levels as the flow reaches more distal muscle. Graph B shows the ratio of retroperfused and baseline fluorescence at each location, in which the dotted line indicates the ratio of peak flow rates in retroperfusion and forward flow (0.44).

Determine the effects of retroperfusion on an acute hindlimb ischemia canine model.

To test whether the reverse flow actually benefited the ischemic tissue, blood gas samples were taken throughout the experiment at pre-occlusion ($n = 6$), post-occlusion 1 hour ($n = 5$), post-occlusion 2 hour (2-3 hours) ($n = 4$), and after retroperfusion ($n = 4$). Graph A of Figure 4.9 shows the oxygen count of the outflow blood (taken from Catheter A) decreasing during injury and trending back towards baseline levels after retroperfusion in which the differences in inflow and outflow go

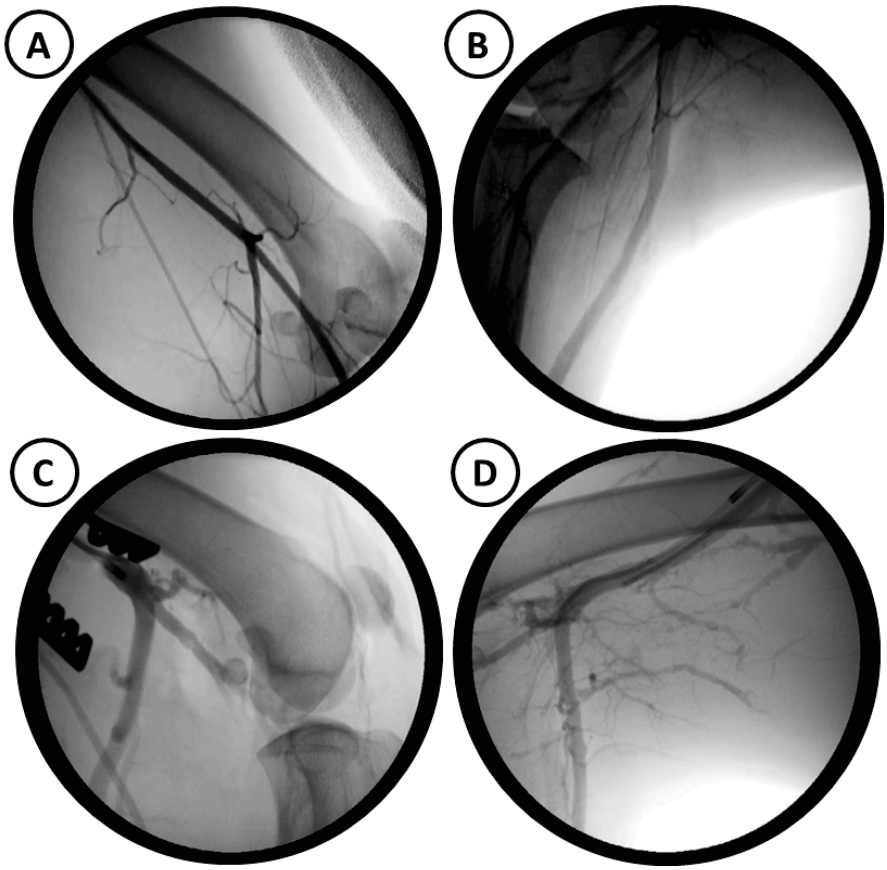

Fig. 4.7. This figure shows (A) an arteriogram at the popliteal artery bifurcation, (B) the injected contrast leaving through the lateral saphenous vein, (C) a venogram at the popliteal vein bifurcation, and (D) both experimental catheters in place.

from $p < 0.001$ at post-occlusion 2 hour to $p < 0.05$ after retroperfusion. Although no statistical difference was shown between post-occlusion 2 hour and after retroperfusion within outflow ($p = 0.462$), a loss of significance was shown between inflow and outflow, indicating the severity of the injury was decreased and thus a positive effect took place. The glucose levels in graph B show an increase in glucose uptake (difference in inflow and outflow values) at post-occlusion 2 hour ($p < 0.05$) and after retroperfusion no statistical difference between inflow and outflow blood samples was detected ($p = 0.350$). Lactate levels (C) show a significant climb at post-occlusion

2 hour ($p < 0.01$) and fall back to no statistical difference value after retroperfusion ($p = 0.226$). Graph D shows the pH of the outflow blood decrease at post-occlusion 2 hour ($p < 0.001$) and climb towards inflow values after retroperfusion ($p < 0.05$).

Table 4.2 displays the remaining noteworthy metabolic data from blood samples through the in-vivo experiments. Partial pressures of carbon dioxide and oxygen, oxygen saturation, and oxygen count all became statistically different at post-occlusion 2 hour, $p < 0.01$, $p < 0.001$, $p < 0.001$, and $p < 0.001$, respectively. pO2 remained at the same significance after retroperfusion and SO2 dropped to $p < 0.01$. (Even though medical oxygen put pO2 into unrealistic values, statistics were still run on the data.) pCO2 and O2's statistical significance dropped to $p < 0.05$ after retroperfusion.

Table 4.2.
Blood Gas Results of Inflow and Outflow Blood Samples

	Pre-Occlusion		Post-Occlusion 1hr	
	Inflow	Outflow	Inflow	Outflow
pCO2 (mmHg)	42.00±3.25	49.83±2.99	40.00±4.36	65.00±11.68
pO2 (mmHg)	501.17±11.63***	119.50±42.70	513.67±34.48***	109.80±68.18
SO2 (%)	101.5±0.07	84.37±.03	101.40±0.00	64.62±11.90
O2ct (mL/dL)	15.63±0.90	12.48±1.08	16.57±0.48	9.68±2.89
	Post-Occlusion 2hr		Retroperfusion	
	Inflow	Outflow	Inflow	Outflow
pCO2 (mmHg)	44.00±5.51**	113.25±1.75	43.67±0.88*	103.00±12.00
pO2 (mmHg)	556.00±5.69***	31.50±3.48	486.00±10.07***	36.00±5.58
SO2 (%)	101.40±0.06***	24.40±3.66	101.30±0.06**	35.48±9.20
O2ct (mL/dL)	15.80±0.65***	4.23±0.70	17.30±2.60*	6.33±2.40

After the data was collected in-vivo, calculations towards an ideal perfusion catheter could be made.

4.4 Theoretical Assessment

Determine the ideal catheter resistance given the hemodynamic data retrieved in in-vivo experiments.

From the hemodynamic data gathered in-vivo, the unknown variable, retro venous vasculature resistance, was used to calculate the ideal catheter resistance. By using Equation 3.2 the pressure and flow of the experimental data dependent on the venous vasculature was used to calculate the ideal catheter resistance. Table 4.3 displays the ideal catheter resistance given an inlet pressure between 80 and 120 mmHg, a catheter output pressure equal to in-vivo data, and inlet flow rates between 100 and 300 ml/min. The target catheter output pressures are boxed. The table shows that when a pressure of 100 mmHg and flow rate of 200 ml/min enter the catheter, a resistance of 0.585 mmHg/ml/min is required for a retroperfusion pressure of around 50 mmHg.

Table 4.3.
Ideal Catheter Resistance Given an Inlet Pressure, a Catheter Output Pressure Equal to In-vivo Data, and Inlet Flow Rates

IDEAL CATHETER RESISTANCE (mmHg/mL/min)											
	Catheter Output Pressure (mmHg)										
Inlet Pressure (mmHg)		17.3	18.5	26.9	36.5	54.2	63.2	68.4	71.7	66.3	
	80	0.856	0.891	0.958	0.978	0.969	0.958	1.007	0.875	1.071	
	90	0.956	0.991	1.058	1.078	1.069	1.058	1.107	0.975	1.171	100
	100	1.056	1.091	1.158	1.178	1.169	1.158	1.207	1.075	1.271	
	110	1.156	1.191	1.258	1.278	1.269	1.258	1.307	1.175	1.371	
	120	1.256	1.291	1.358	1.378	1.369	1.358	1.407	1.275	1.471	
		17.3	18.5	26.9	36.5	54.2	63.2	68.4	71.7	66.3	
	80	0.571	0.594	0.639	0.652	0.646	0.639	0.671	0.584	0.714	
	90	0.637	0.660	0.705	0.719	0.713	0.706	0.738	0.650	0.781	150
	100	0.704	0.727	0.772	0.786	0.780	0.772	0.804	0.717	0.847	
	110	0.771	0.794	0.839	0.852	0.846	0.839	0.871	0.784	0.914	
	120	0.837	0.860	0.905	0.919	0.913	0.906	0.938	0.850	0.981	
		17.3	18.5	26.9	36.5	54.2	63.2	68.4	71.7	66.3	
	80	0.428	0.445	0.479	0.489	0.485	0.479	0.503	0.438	0.535	
	90	0.478	0.495	0.529	0.539	0.535	0.529	0.553	0.488	0.585	200
	100	0.528	0.545	0.579	0.589	0.585	0.579	0.603	0.538	0.635	
	110	0.578	0.595	0.629	0.639	0.635	0.629	0.653	0.588	0.685	
	120	0.628	0.645	0.679	0.689	0.685	0.679	0.703	0.638	0.735	
		17.3	18.5	26.9	36.5	54.2	63.2	68.4	71.7	66.3	
	80	0.342	0.356	0.383	0.391	0.388	0.383	0.403	0.350	0.428	
	90	0.382	0.396	0.423	0.431	0.428	0.423	0.443	0.390	0.468	250
	100	0.422	0.436	0.463	0.471	0.468	0.463	0.483	0.430	0.508	
	110	0.462	0.476	0.503	0.511	0.508	0.503	0.523	0.470	0.548	
	120	0.502	0.516	0.543	0.551	0.548	0.543	0.563	0.510	0.588	
		17.3	18.5	26.9	36.5	54.2	63.2	68.4	71.7	66.3	
	80	0.285	0.297	0.319	0.326	0.323	0.319	0.336	0.292	0.357	
	90	0.319	0.330	0.353	0.359	0.356	0.353	0.369	0.325	0.390	300
	100	0.352	0.364	0.386	0.393	0.390	0.386	0.402	0.359	0.424	
	110	0.385	0.397	0.419	0.426	0.423	0.419	0.436	0.392	0.457	
	120	0.419	0.430	0.453	0.459	0.456	0.453	0.469	0.425	0.490	

Realistic Inlet Flow Rates (mL/min)

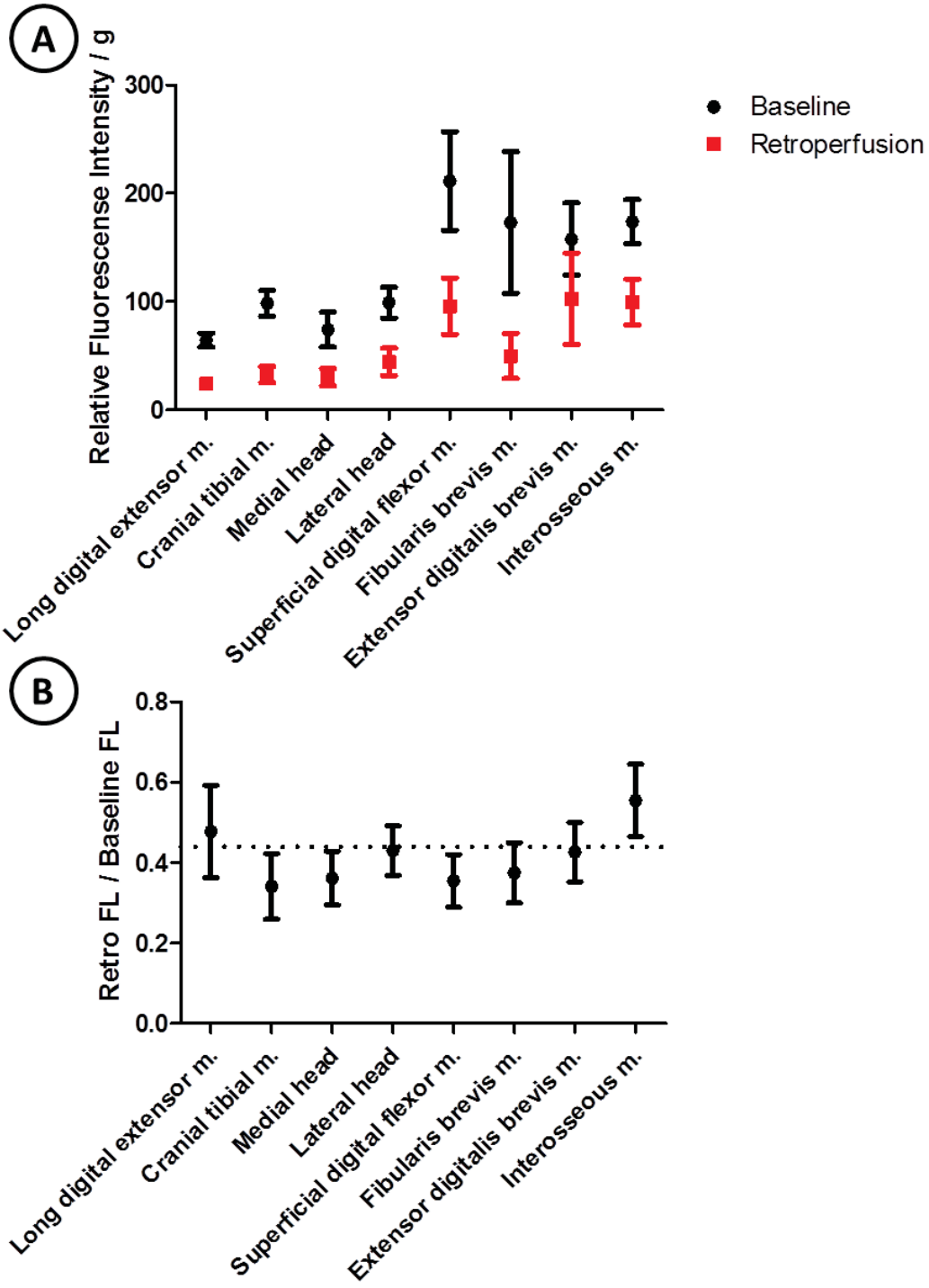

Fig. 4.8. This figure shows (A) the relative fluorescence intensity per gram tissue of the forward perfusion territory (baseline) and retrograde perfusion territory (retroperfusion) at various distal limb muscles and (B) the ratio of perfusion fluorescence. The dotted line indicates the ratio of peak flow rates in retroperfusion and forward flow (0.44).

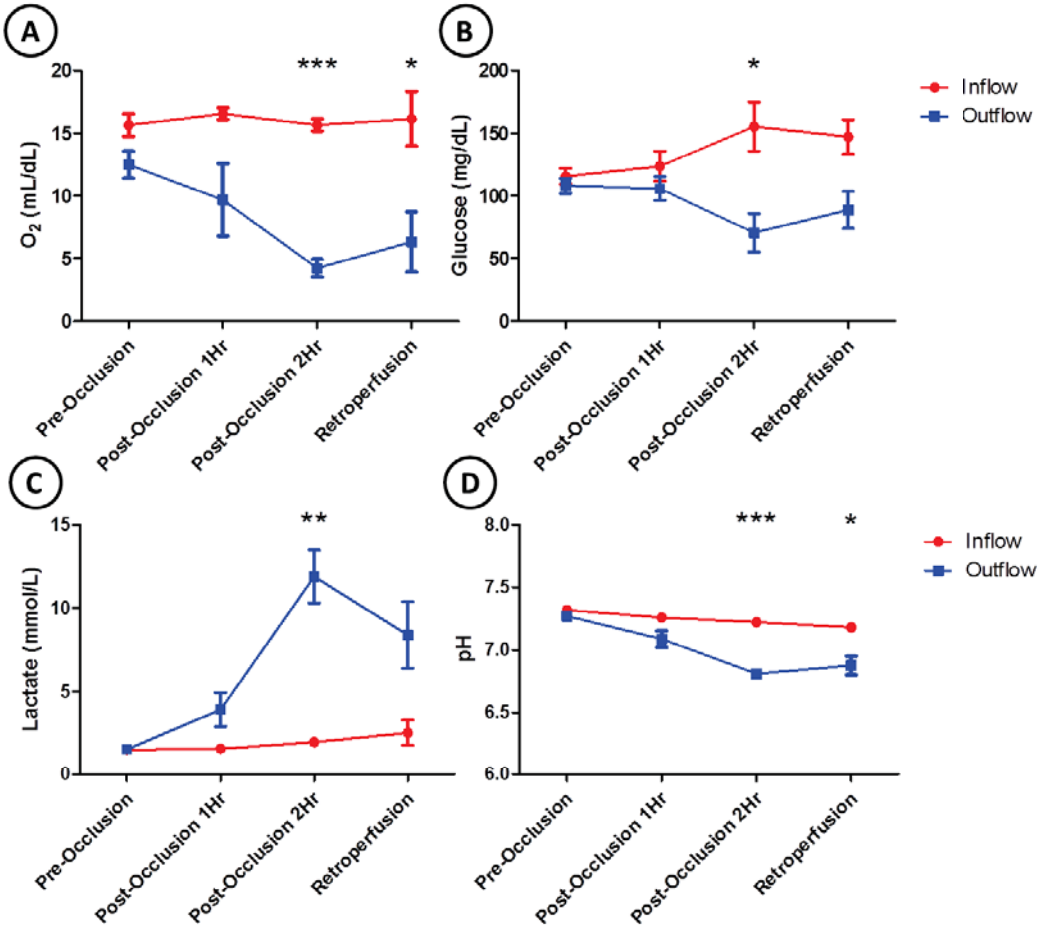

Fig. 4.9. This figure shows the metabolic results of blood samples from inflow and outflow blood taken at pre-occlusion, post-occlusion 1hr, post-occlusion 2hr, and after retroperfusion. (A) is the oxygen content, (B) glucose, (C) lactate, and (D) pH. *,**,** indicate $p < .05$, $p < 0.01$, and $p < 0.001$, respectively, for inflow and outflow values above the specified event.

5. DISCUSSION

Globally, over 200 million people suffer from peripheral arterial disease [44] and approximately 1 million amputations are performed every year [45]. In the United States these numbers reach 8 to 12 million [12] and 185,000 [46], respectively. Over half of all amputations performed are due to vascular disease [45, 46], particularly critical limb ischemia, the most severe form of PAD, of which 5-10% of typical claudicants will acquire within 5 years of diagnosis [10]. Within the first year of of CLI diagnosis, 30% require a major amputation and 25% will die [10, 47]. Thus, the need for limb salvage is clearly a concern for all stages of peripheral arterial disease.

Revascularization techniques for these amputee-fated patients have been explored sporadically over the last century and mainly occupied by reversed flow techniques [19, 20, 24, 25, 29, 30, 33–37]. Initially, flow reversal was explored by connecting an artery to its neighboring vein in-situ in an attempt to restore flow in the ischemic areas [19,24,26]. Typical shortcomings were from valve competency prohibiting distal flows [19, 24, 25] to uncontrollable edema [25] and some ended in heart failure due to the high cardiac output as a result of venous-venous shunting [24, 27, 38]. Recent clinical studies [33–36] excise an accessory vein, strip it of its native valve, attach to it a patent artery, and attach to a major foot vein to ensure distal flow. Although this approach is much more invasive and timely, the results have shown high salvage rates.

It was our belief that the concerns of both retroperfusion techniques could be overcome in a minimally invasive/catheter based approach in which the catheter itself provides a engineered specified resistance that avoids edema and the perfusion location allows for valves to be passable and flow to reach distally. This approach merges the advantages of both retroperfusion techniques without the repercussions of each of the techniques.

Our study was broken up into a series of phases: a theoretical assessment, an ex-vivo proof of concept, an in-vivo validation of the ex-vivo results and gathering of data, and final calculations of an ideal catheter. The theoretical assessment broke up the study in an engineering approach, which revealed what unknown parameters were needed for an ideal catheter. The ex-vivo experiments where done to show where and what flows are possible in retroperfusion, to further indicate what perfusion location to explore in in-vivo, and what hemodynamics we might expect at that location. The in-vivo experiments addressed the hemodynamics of the perfusion location under injury, where the reversal flow actually went compared to forward arterial blood flow, and whether the retroperfusion showed any positive signs of reversing the injury. The hemodynamic data gathered in-vivo was then added to the theoretical assessment to calculate the ideal catheter resistance needed to obtain a perfusion pressure that will not result in edema.

5.1 Determine how the Catheter Resistance Relates to the Physiological System.

The theoretical basis of the study gave direction for what experiments needed to be done to support the overall hypothesis.

By examining the clinical setting of the catheter in series with the venous vasculature, we could easily solve for the variables of the system analytically. Though some studies have put great detail into representing the vascular system as an electrical circuit and parameter characterizations [48–52], our model was only intended to be used as a tool to pull out approximate relationships to guide the study into further experiments and not as an absolute characterization of the system.

Table 4.1 shows each parameter, whether it is known, where it is located, and the specifications of each. The $Pressure_{Input}$ would come from the most distal satisfactory artery and supply the catheter with the arterial inputs. The input pressures from the artery ($IP_{Catheter}$) were expected to be in range of femoral artery supine

and standing values, between 90-150 mmHg [1]. For femoral artery flow rates, it has been shown in healthy humans to range from 300-400 ml/min [53–56] when resting in supine position. Resting values were shown to be the nearly the same for intermittent claudication and critical limb ischemia 436 and 307 ml/min, respectively [56], and 401 ml/min for all PAD patients [55]). Output pressure of the catheter ($OP_{Catheter}$) in the venous system was targeted between 40-60 mmHg, because it has been shown that retrograde venous pressures greater than 60 mmHg damage venules [57]. Our lab has previously suggested to target a pressure of 50 mmHg, the mean of typical arterial and venous pressures, thus 40-60 mmHg was the targeted output pressures [22, 58]. The last known parameter, vasculature output pressure ($OP_{Vasculature}$) was assumed to be 0 mmHg for simplicity. The vasculature output pressure was considered to be located where the pressure is equal to 0 mmHg rather than the venous end of the capillary bed. This assumption allows for the vasculature to represent a much more complex network.

From here, the only parameters left were the unknown variables: catheter resistance ($R_{Catheter}$) and venous retro-vasculature resistance ($R_{Vasculature}$). In order to determine the ideal catheter resistance needed to obtain the target output pressures, the venous retro-vasculature resistance was needed because the pressure drop across the catheter is relative to the resistance of the vasculature. In other words, if the resistance of catheter is much greater than the resistance of the vasculature, then the catheter will take up nearly all the pressure leaving little output pressure and if vice versa the catheter will maintain nearly all the pressure from the inlet thus resulting in very high pressures in the venous system. Neither case is ideal because, according to Zweifach 15 to 40 mmHg of pressure is needed at the capillary level for flow and nutrient exchange, but pressures greater than 40 mmHg results in sudden edema in the capillary bed [8].

The venous retro-vasculature resistance was determined experimentally as the slope of a pressure flow curve. Once a value was given to this variable the ideal catheter resistance resulting in the target output pressures was solved for.

5.2 Determine the Resistance of the Venous Retro-Vasculature Most Suitable for Effective Retroperfusion.

5.2.1 Determine Whether Flow Reversals are Possible.

Because previous retroperfusion efforts had issues rendering the valves incompetent, exploration of if and where flow reversal were even possible was required. Ex-vivo canine hindlimbs were the initial experimenting platform due to their abundant supply, similiar peripheral vascular system to humans, and their vascular system being easily attainable [25, 29].

An early attempt at retroperfusion looked as if flow reversal would not be possible. Figure 5.1 shows the massive change in pressure with little changes in flow when flow was fed into the femoral vein retrogradely as opposed to a near one to one relationship from forward flow in the femoral artery. This quick experiment was a quick reminder from literature that very proximal venous valves are extremely difficult to render incompetent to flow [19].

A brief feasibility check was performed in-vivo to determine if the mighty proximal valves were passable at all. Figure 5.2 shows the valves being passed with a guidewire at the iliac level to midway of lateral hindlimb. The contract injections show immediate back flow towards the heart in images A-C. It was concluded that the venous valves were passable retrogradely, but a hydrophilic guidewire and forward flow were considered necessary to reach distal veins.

5.2.2 Determine if the Retroperfusion Hemodynamics is Location Dependent.

Once the femoral level valves became easy to routinely pass we then began to gather hemodynamic data throughout the limb. A 'proximal' location (popliteal vein bifurcation) was explored, a 'midway' location (lateral saphenous vein bifurcation), and a 'distal' location (vneous dorsum pedis). Because the hemodynamics were assumed to be location dependent, these three locations were investigated.

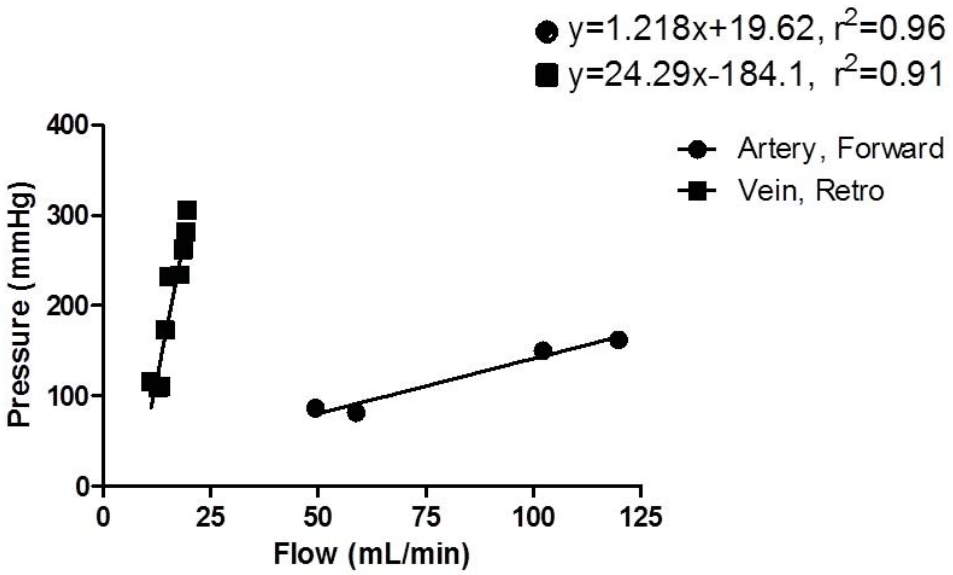

Fig. 5.1. This figure shows an early attempt at retroperfusion in the femoral vein compared to forward perfusion at the femoral artery.

The qualitative results shown in Figure 4.2 display the shunting effects at the midway and distal location. Figure 5.3 clearly shows the major escape routes the flow can take when the flow is supplied in the foot. The quantitative results shown in Figures 4.3 and 4.4 indicate no statistical difference between the slopes but the distal location does have a significantly different y-intercept. The slope was interpreted as the resistance of the system (venous vasculature) due to simplicity of the system design, in which others have considered the pressure-flow relationship as resistance [49,50,59] or vascular impedance [60] for arterial antegrade flow. The y-intercept was interpreted as the equilibrium pressure when no flow is present, similar to the mean circulatory filling pressure, or the residing pressure in the vasculature once the heart stops beating [1,52]. Because the y-intercept is significantly less for the distal location, we assume this is due to less compliant veins being filled at the distal location. Thus less collapsed vasculature to fill would result in a lower y-intercept [51,59]. Antegrade arterial pressure-flow studies have looked into this 'zero-flow pressure' as the effective

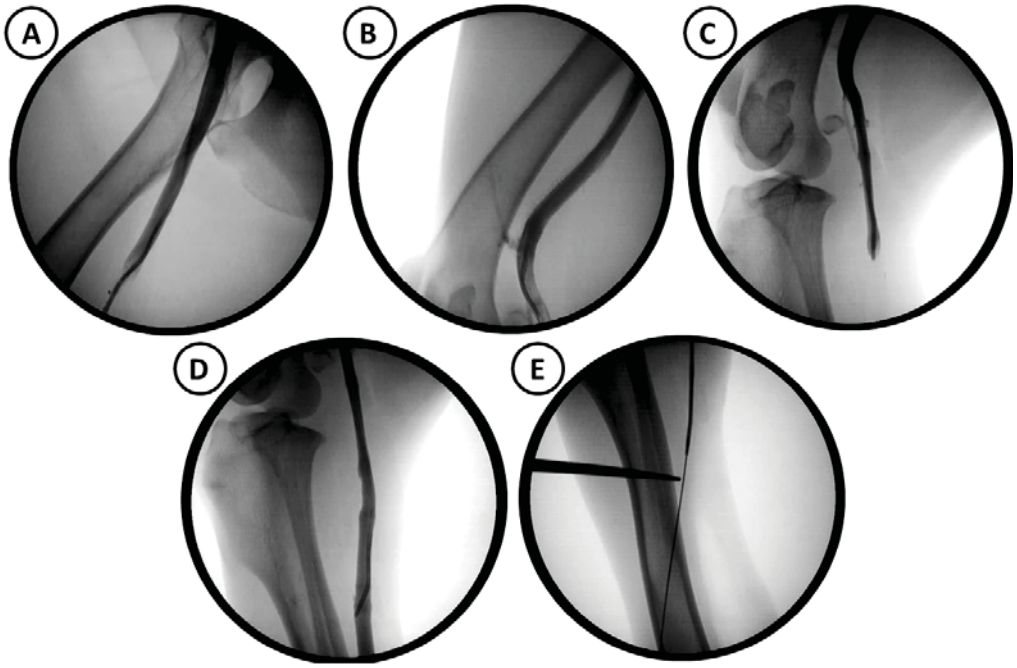

Fig. 5.2. This figure shows the distal venous system of a canine hindlimb being accessed in-vivo. (A) shows the iliac/femoral region, (B) the popliteal region, (C) the distal femoral caudal region, (D) the lateral saphenous region, and (E) the cranial lateral saphenous region.

downstream pressure to arterial flow that onsets vascular waterfall [51, 52, 59, 61], the pressure height that must be reached before any subsequent flow is met or also known as the critical closing pressure. In our study is it assumed that the antegrade critical closing pressure is similar to our retrograde y-intercept of mean circulatory filling pressure.

For simplicity, because the proximal and midway locations were not statistically different their data was combined to represent a new combined proximal data set.

Fig. 5.3. This figure shows the distal shunting effects of flow.

5.2.3 Determine What Location Seems Most Promising for Effective Retroperfusion.

The hemodynamics did not prove to be as location dependent as we originally thought. Between the two distinct locations of the popliteal vein bifurcation and dorsum pedis, the proximal location indicated favorable qualitative characteristics as an in-vivo perfusion site since the distal location clearly showed immediate venous-venous shunting. Clinically, if too much shunting occurs it is assumed that little to no blood will reach the microvasculature to salvage the ischemic limb [27] and the body will compensate by increasing cardiac output in which heart failure can occur [24, 27, 38]. To investigate the proximal location more thoroughly, the pressure wire was kept distal past the perfusion location to detect distal pressures. Figure 5.4 shows the pressures reached at the midway, distal, and very distal locations were

relative to the pressure at the tip of the catheter at the popliteal vein bifurcation. Because pressures were being reasonably maintained past the tip of the catheter it was assumed that a reasonable amount of the flow was reaching the same locations. With these encouraging results, it was hypothesized that the popliteal vein bifurcation would make a successful retroperfusion location in-vivo since flows were indicated past the site of perfusion with no signs of venous-venous shunting. A possible explanation for no signs of venous-venous shunting could be due valve direction that plays a part in flow movement, such that perforating veins move flow from superficial to deep and prevent deep reflux into the superficial system [3,27,62]. By the valves in perforating veins preventing deep to superficial venous flow, one could assume that at the popliteal bifurcation, being as it is part of the deep system, perforating veins would act in favor of continual deep reversed flow.

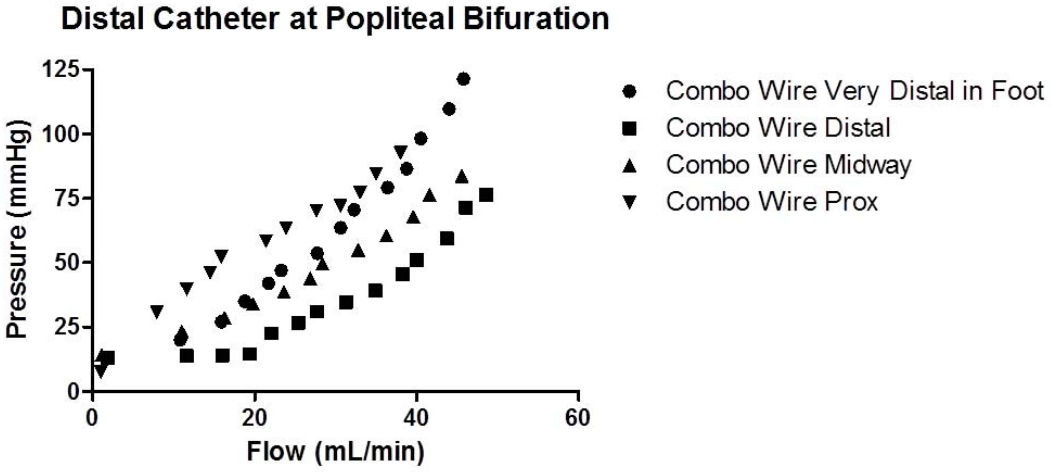

Fig. 5.4. This figure shows evidence of distal pressures when the retroperfusion site is at the popliteal vein bifurcation.

5.3 Determine the Resistance of the Venous Retro-Vasculature and Characteristics of Retroperfusion In vivo.

A hindlimb ischemia model was performed prior to in-vivo retroperfusion. The injury model displayed in Figure 3.4 needed to be aggressive since all the experiments were done acutely. Threshold for muscle ischemia recovery has been claimed to be between 2-6 hours [63–65] and several studies have shown extreme metabolic effects after 3 hours of occlusion [66], thus our occlusion time was between 1-3 hours with ultrasound and direct angiography verification [67, 68].

It has also been confirmed that multiple occlusions closer to the aorta produce more profound ischemic effects than single distal ligations (e.g. femoral level) [68, 69] in which Rosenthal showed collateral compensation within the first hour of femoral artery occlusion in canines [70]. Despite clinical evidence of severe ischemia, even ligatures of rat common iliac, femoral, and branching on a single limb have shown maintenance of blood flow in the ischemic limb [71]. In addition, bilateral ligations have also shown to create a more severe ischemic limb in a rat model [68]. It is typical for rat and canine models to need more aggressive limb injuries due to their abundant collateral network compared to a rabbit or pig model whom show a human-like absence of limb collateral network [68]. An adverse effect of placing the retroperfusion catheter sheath in the distal vena cava caused arterial and venous occlusions which was thought to attribute to the severity of the ischemia [67]. Ligations in the non-experimented leg and terminal aorta were made to prevent any possible immediate collaterals to the experimental leg [68, 72, 73] and thus no control leg was made in the experiments. All major native collaterals were intended to be avoided to ensure all effects post-retroperfusion could be confirmed by retroperfusion and not by collateral compensation. This avoidance was considered important since the patients being treated are not likely to have major collateral compensation in their poorly perfused distal limb. To capture noncollateral effects, one group looking at ischemic metabolic levels went as far as to take measurements immediately after killing the animal to avoid confusion of collateral effects on muscles ischemia [74], a solution that would not

make sense here for in-vivo data collection. The acute experiments were performed on mongrel dogs with 10 weeks of venous hypertension. The state of the dogs were considered ideal since their venous system was preconditioned to higher pressures and wall thickening had already occurred [20, 75]. This is the vascular state that the veins clinically will become prior to full implantation by allowing distal catheter flow to travel antegrade or retrograde for several weeks before closure at the tip for only distal flows.

5.3.1 Determine the Active Hemodynamics at the Retroperfusion Site.

Because retroperfusion would only take place in an ischemic limb and flow will only occur when a pressure difference exists, an ischemia model was needed to gather realistic retroperfusion data.

The popliteal vein bifurcation was chosen to be the retroperfusion site because of the ex-vivo results, the most successful in-situ flow reversal as previously been the popliteal vein bifurcation [29,30], and because it was previously shown that the venous valves did not affect retro-filling at this location [76]. After the injury had set for 1-3 hours, retroperfusion was performed for approximately one hour. Figure 4.5 shows the raw data from each animal and then compared to the ex-vivo results. The significant difference in the y-intercepts are displayed in Figure 4.6. A similar difference has been shown between instantaneous and steady-state pressure-flow relations at femoral artery level [49, 59, 61] in which the steady state allows for arteriole compensation as shown by the curvature of the response and instantaneous captures the true physical resistance typically shown as linear [49, 59, 61, 77, 78]. However, here we collected data points every 30-45 seconds for ex-vivo and every 1-3 minutes in-vivo, making our pressure-flow data steady state. The slight curvature to the in-vivo data could be explained by the vascular response to the retro flows and pressures but for ex-vivo no vascular response could be made in the dead tissue hence the non-curvature relationship.

The y-intercept difference is again assumed to be characterized by the filling pressure. In the ex-vivo experiments the veins were collapsed causing more pressure needed to get any resulting flow, but in in-vivo experiments little pressure is needed to distend the veins and result in flow of which our value relates to literature MCFP [1]. Although the y-intercepts are significantly different, the slopes indicate that venous retro-vasculature resistance are similar from the passive to active state. Aside from the curvature of in-vivo data, this observation could suggest that, acutely, the venous retro-vasculature resistance has no active properties affecting the overall resistance of the periphery.

The hemodynamic data of the retro venous system collected in-vivo provided the missing information needed to calculate the catheter resistance that limits the perfusion pressure to a healthy range.

5.3.2 Determine the Perfusion Territory of Venous Reversed Flow Compared to Arterial Forward Flow.

Fluorescent microspheres were injected to gather information as to where the retro flow actually went during retroperfusion. If no flow was shown to make it to ischemic muscles throughout the limb, support of the actual device would be limited. The perfusion territory of baseline of forward arterial flow was compared to the perfusion territory of retroperfusion of reverse venous flow. Two very different fluorescent microspheres were injected for each case to ensure no spillover effect [71] and the overall methods of injection and analysis followed that of the Fluorescent Microsphere Resource Center [41, 42].

The relative levels of the retroperfused fluorescence in Figure 4.8 trends similar to the baseline fluorescence at a respective location with a slight increase in levels as the flow reaches more distal muscle (further down the x-axis). The ratio of retroperfused and baseline fluorescence at each location hovers around the dotted line which indicates the ratio of peak flow rates in retroperfusion (37 ml/min) and forward venous

flow (85 ml/min) of 0.44. We assume if higher flow rates were reached, the levels of retroperfusion would increase as well. It has been suggested that retro-flow rates of 60 ml/min are needed to salvage the limb [79], though here our max rates only reached near 40 ml/min, a note that will weigh into the chronic validation model and the targeted flows.

The slight upward increase in fluorescent levels in the more distal muscle is thought to be due to the perfusion territory becoming more localized as the flow makes its way to the distal limb, in which this localization is considered necessary for flow in the foot [20].

5.3.3 Determine the Effects of Retroperfusion on an Acute Hindlimb Ischemia Canine Model.

To evaluate if retroperfusion at the chosen perfusion site had any metabolic effect on the ischemic hindlimb, blood samples were retrieved throughout the experiment before and after occlusion and after retroperfusion. The blood gas results shown in Figure 4.9 indicate onset of anaerobic glycolysis at post-occlusion 2 hour due to the significant decrease in oxygen count, significant increase in glucose uptake and lactate production, and significant drop in pH [74]. Younger explained that high lactate levels could be misleading if the site of retrieval is very close to ischemia induced site in which extreme local effects would outway the effects of musculoskeletal hypoperfusion [80]. This was not a concern of ours since the occlusion site was the aortic bifurcation and retrieval was at the popliteal level thus the lactate levels was assumed to do to musculoskeletal hypoperfusion.

Our baseline lactate levels, shown is Figure 4.9, were similar to another animal study [81]. Peak lactate levels were similar to previous animal studies when skeletal muscle ischemia was induced by 1 and 6 hours of arterial occlusion [82, 83], respectively, and immediate death [74]. Specifically, Kabaroudis showed no significant difference in canine popliteal venous lactate levels between 1, 6, and 12 hours of femoral

artery occlusion and very similar glucose levels for baseline and peak injury (their 12 hour, our 2 hour) [82]. The difference in occlusion times to metabolic severity is thought to be caused by the difference in the occlusion methods, in which ours was at the aortic bifurcation.

Due to the lack of oxygen, anaerobic glycolysis was the only long term energy mechanism that could take place [74,84]. Glucose levels, shown is Figure 4.9, dropped in outflow due to uptake in glycolysis and lactate levels increased due to fermentation in which lactic acid is produced in order to continue ATP production in glycolysis. The lactic acid buildup then decreased pH levels in the outflow. After approximately one hour of retroperfusion, the signs of anaerobic glycolysis decreased, though not significantly. However, Figure 4.9 shows the oxygen count and pH levels remained significantly different from inflow ($p < 0.05$ v. $p < 0.001$) when glucose and lactate levels were no longer significantly different from the inflow levels, suggesting a significant trend back to baseline levels.

The oxygen levels in Table 4.2 shows the metabolic response to partial pressures of carbon dioxide and oxygen, oxygen saturation, and oxygen count. Here, even though the outflow levels of each trended back towards baseline values, although their levels remained statistically different to inflow.

Evaluation of retroperfusion post-injury was critical to prove the potential of the perfusion site. By showing the signs of anaerobic glycolysis were somewhat reversed post-retroperfusion, we are hopeful that this observation will continue and strengthen in a chronic peripheral arterial disease model.

5.4 Determine the Ideal Catheter Resistance Given the Hemodynamic Data Retrieved in In-vivo Experiments.

The in-vivo experimental pressure-flow data provided us with the necessary data to calculate the ideal catheter resistance needed chronically and clinically. The flows rates experienced in-vivo were much lower than those expected chronically and clin-

ically from the arterial input when the catheter will have native inflows from the femoral artery or higher (our max reached retro flows of 40 ml/min vs. canine femoral artery flows of 60-140 ml/min [25, 28, 85, 86] vs. human femoral artery flows of 300-450 ml/min for normal and PAD patients [53–56]). Also, inflow pressures are expected to be different as well (canine femoral artery pressure of 130 mmHg [70, 85] vs. human femoral artery pressure of 100 mmHg [1]). Because of this, a few extra manipulations were needed to calculate the catheter resistance, shown in Section 3.4.

A table of ideal catheter resistances given an input/arterial pressure, target perfusion pressures, and arterial flow rates was made for reference for the optimal catheter design of which would be used in clinical setting (Table 4.3). The input arterial pressures and flow rates were given a range because not all the pressure and flow is planned to be diverted into the retroperfusion catheter thus a range was examined. The middle pressures were boxed because they are near the target output pressures. The table is intended to be used as a tool for a final catheter design. For example, if the design engineer knows the flow rate will be in a finer fixed range, then the catheter resistances can be confined to a more precise value and thus the likeliness of the device success can be theoretically more supported.

6. CONCLUSIONS

Being able to indicate very distal reversed flows and show signs of acute ischemia reversal by retroperfusion at a specific perfusion location validates further efforts of this proof of concept. In order to be confident in this method of perfusion, a chronic study is critical to prove its potential. In the chronic model a shunting device of ideal resistance calculated in this study will take the place of the extracorpeal circuit and will be directly implanted from artery to vein. The device itself will account for the optimal pressure drop and retrogradely perfuse at nearly a constant pressure. It is expected that the retroperfusion effects will hold true past any acute responses and adequate collateralization will form to reroute the blood to and from the ischemic sites. If the chronic results are promising, severe peripheral arterial disease patients will finally have a treatment option in which they can keep their limbs.

6.1 Limitations and Future Work

The major limitations of the study mainly fall on how all the in-vivo effects came from acute experiments rather than chronic experiments. Clearly, the next step of the study is to take the findings found here throughout the study and apply them to a chronic animal model.

Catheter resistance, and location and success of the retroperfusion device was demonstrated here in the deep system at the popliteal vein bifurcation. Possibility of reversed flow here, how to reach this location retrogradely, and why this location was most promising was shown in this study, as supported by no signs of shunting, previous chronic success, detection of distal flows in ischemic muscles, and acute indication of reversed injury through reversed flow. Although many findings were made, a few limitations of the study include the dynamics of blood pressure and

flow and its overall effect on the catheter, further validation of retroperfusion success, time to develop injury, time to observe retroperfusion effects, and ischemic animal model not being specific for critical limb ischemia. In addition, more time could have been spent in the early stages of the study, further supporting the retroperfusion location, however the ex-vivo studies were done purely to guide the more meaningful in-vivo experiments and work out experimental hurdles rather than spending time characterizing 'dead tissue'.

Dynamics of the System. It is important to consider the hemodynamic effects on standing compared to resting supine levels, in which all previously cited literature and parameter values are from resting supine. Even though all the pressure and flow collected throughout the study all came from pulsatile data (catheter outflows pressures had a mean peak to peak value of 14 mmHg, a pulsatility between artery and vein, Figure 1.3 [1]), only the mean values were plotted and referred to of which came from resting supine position. For femoral artery flow rates, it has been shown in healthy humans to range from 300-400 ml/min [53–55] when resting in supine position and to drop to ∼200 ml/min when standing [56]. Resting values have been shown to be the nearly the same for intermittent claudication and critical limb ischemia, 436 and 307 ml/min, respectively, and 401 ml/min for all PAD patients [55], but when standing intermittent claudicants drop to 220 ml/min near healthy standing range whereas CLI patients increase to nearly 500 ml/min. Femoral level pressures in healthy humans increase to 150 and 60mmHg for artery and vein from approximately 90 and 5 mmHg, respectively [1], although these values are reduced to near resting supine after about ten steps [3]. Effects of catheter resistance should be examined at these 'active' cases to determine whether edema can be avoided during standing and/or walking with the device implanted or if the implant will only result in limb salvage at rest. By using part of the venous system as a perfusion route to the distal limb this takes away part of the venous systems's ability to control for pressure, thus it is assumed that pressure will not be as easily regulated. It is also assumed that blood flow will be difficult to regulate prior to venous arterialization and angiogenesis

since arterioles are the main regulators of flow and won't have major contribution until either of the two events occur. However, limb salvage at rest in itself can avoid amputation but avoidance of complications and continued limb salvage during standing/walking could make the device much more valuable and/or explain successes or failures in previous flow reversal attempts.

Further Validation of Acute In-Vivo Experiments. To add a layer of validation of retroperfusion in the acute in-vivo studies, more ischemia and flow analysis could have been done. Muscle biopsies for ischemia detection would have confirmed the level of injury throughout the skeletal muscles in the study and again after retroperfusion to confirm if metabolic levels were reversed and to support the outflow blood samples taken at the popliteal level. Biopsies were taken throughout the study but were not analyzed for this thesis. Planned analysis methods include NADH-tetrazolium [83] and hematoxylin and eosin staining [87] for ischemia detection and edema detection, respectively. Surface pO2 (or transcutaneous pO2, TcpO2) levels would have also added a layer of acute retroperfusion success as others have shown likelihood of wound healing is promising when TcpO2 is >40 mmHg, and unlikely when <20 mm Hg [16]. This was attempted during the study but results were unreliable due to lack of equipment sensitivity.

Future Endpoints. Analysis methods for chronic study should include a combination of qualitative functional scoring similar to Tarlov scale [67], metabolic detection of outflow lactate and/or glucose [68, 81, 82], pulse detection in toes [24, 38], flow/perfusion detection (using laser doppler perfusin imaging and/or angiography [67–69]), oxygen detection (using transcutaneous oximetry), pressure detection (using ABI index and/or TBI index) throughout the study [16] and flow/perfusion detection of collaterals and capillaries (using microspheres [71] and/or immunohistochemical stainings [67–69]) collected at the end of the study.

Animal Model Criticism. Like nearly all PAD animal models, our model was not specific for the targeted disease [62, 68, 72, 88]. However, for our acute study, the aggressiveness of the injury showed metabolic ischemic effects within the critical

ischemia time of 2-6 hours [63–65] relative to literature values. However, no reversed flow studies examined the ischemic metabolic levels prior to experimental reversed flow, either nothing [25, 29] or only pressure ratios, pulse detection, oxygen tension, and surface pH [24] were examined. Our occlusion time allowed us to get initial insight of the response of controlled reversed flow with ensured ischemia. Other studies that produced irreversible injury applied flow reversal immediately [25, 29] or only allowed 30 minutes of stabilization [24] due to the severity of the injury and then had reversed flow for 30 minutes [24] for detection of acute effects or others waited 10-14 days for chronic effects [25,29]. Some studies performed no type of injury before observing reversed flow effects [28, 86, 89] or performed minute occlusions for a couple of minutes and then observed results [85]. Ours looked at the acute ischemic response and retroperfusion response. Compared to other reverse flow studies, we allowed longer time for the injury to set before observing retroperfusion effects, arguably making our results more relevant.

Chronic Animal Model of PAD. The animal model for chronic experiments should be taken into great consideration. A model that avoids native collateral flow is critical in order to validate the retroperfusion catheter. Because most studies look at ischemia models to study collateral formation our model must avoid this. Rosenthal showed the sensitivity of collateral formation when systemic pressure was halved, even when no occlusion was set in place, a compensation that severe PAD patients lack [70]. Because severe PAD patients have issues to flow compensation a model that supports this would be futile in validation of the study. It is reasonable to have multiple levels of validating chronic studies with alterations in the animal model more similiar to the disease itself. A model that shows irreversible ischemia could be a first step, like the animal model developed by Graham [29, 30]. A more validating animal model that would avoid using only simple occlusions and provide some type of endothelial dysfunction like that of patients with critical limb ischemia through addition of hyperlipidemia or diabetes model [62, 68, 88] would be an more ideal animal model to test the device in prior to clinical trials.

REFERENCES

REFERENCES

[1] W. F. Boron and E. L. Boulpaep, *Medical physiology. A cellular and molecular approach. Saunders.* Elsevier Science, Philadelphia, 2009.

[2] D. A. Rubenstein, M. D. Frame, and W. Yin, *Biofluid Mechanics: An Introduction to Fluid Mechanics, Macrocirculation, and Microcirculation.* Academic Press, 2011.

[3] M. H. Meissner, G. Moneta, K. Burnand, P. Gloviczki, J. M. Lohr, F. Lurie, M. A. Mattos, R. B. McLafferty, G. Mozes, R. B. Rutherford *et al.*, "The hemodynamics and diagnosis of venous disease," *Journal of vascular surgery*, vol. 46, no. 6, pp. S4–S24, 2007.

[4] "The venous system within the cardiovascular system," http://www.urgo.co.uk/260-the-venous-system-within-the-cardiovascular-system, 2014, [Accessed October 28, 2014].

[5] J. D. Humphrey, *Cardiovascular solid mechanics: cells, tissues, and organs.* Springer, 2002.

[6] "Lab 3: heart and vessels," https://www.studyblue.com/notes/note/n/lab-3-heart-and-vessels/deck/2096796, 2014, [Accessed October 28, 2014].

[7] K. B. Chandran, S. E. Rittgers, and A. P. Yoganathan, *Biofluid mechanics: the human circulation.* CRC Press, 2012.

[8] B. W. Zweifach, "The structural basis of permeability and other functions of blood capillaries," in *Cold Spring Harbor Symposia on Quantitative Biology*, vol. 8. Cold Spring Harbor Laboratory Press, 1940, pp. 216–223.

[9] "Systemic blood pressure (outline)," http://news.genius.com/Human-physiology-systemic-blood-pressure-outline-annotated-note-1655693, 2014, [Accessed October 28, 2014].

[10] L. Norgren, W. R. Hiatt, J. a. Dormandy, M. R. Nehler, K. A. Harris, and F. G. R. Fowkes, "Inter-society consensus for the management of peripheral arterial disease (tasc ii)," *European Journal of Vascular and Endovascular Surgery*, vol. 33, no. 1, pp. S1–S75, 2007.

[11] R. P. Choudhury, V. Fuster, and Z. A. Fayad, "Molecular, cellular and functional imaging of atherothrombosis," *Nature reviews Drug discovery*, vol. 3, no. 11, pp. 913–925, 2004.

[12] "Facts about peripheral arterial disease (p.a.d.)," http://www.nhlbi.nih.gov/health/educational/pad/docs/pad-extfctsht-general-508.pdf, 2006, [Accessed October 30, 2014].

[13] "Peripheral arterial disease (pad) fact sheet," http://www.cdc.gov/dhdsp/data-statistics/fact-sheets/fs-pad.htm, 2013, [Accessed October 28, 2014].

[14] J. S. Berger and W. R. Hiatt, "Medical therapy in peripheral artery disease," *Circulation*, vol. 126, no. 4, pp. 491–500, 2012.

[15] S. Kinlay, "Outcomes for clinical studies assessing drug and revascularization therapies for claudication and critical limb ischemia in peripheral artery disease," *Circulation*, vol. 127, no. 11, pp. 1241–1250, 2013.

[16] P. W. Wennberg, "Approach to the patient with peripheral arterial disease," *Circulation*, vol. 128, no. 20, pp. 2241–2250, 2013.

[17] "About peripheral artery disease (pad): American heart association," http://www.heart.org/HEARTORG/Conditions/More/PeripheralArtery Disease/About-Peripheral-Artery-Disease-PAD-UCM-301301-Article.jsp, 2014, [Accessed October 28, 2014].

[18] "Peripheral arterial disease of the legs - surgery: Web md," http://www.webmd.com/heart-disease/tc/peripheral-arterial-disease-of-the-legs-surgery, 2014, [Accessed October 28, 2014].

[19] D. E. Szilagyi, G. D. Jay, and E. D. Munnel, "Femoral arteriovenous anastomosis in the treatment of occlusive arterial disease," *AMA archives of surgery*, vol. 63, no. 4, pp. 435–451, 1951.

[20] X. Lu, M. Idu, D. Ubbink, and D. Legemate, "Meta-analysis of the clinical effectiveness of venous arterialization for salvage of critically ischaemic limbs," *European journal of vascular and endovascular surgery*, vol. 31, no. 5, pp. 493–499, 2006.

[21] R. Heimbecker, V. Thomas, and A. Blalock, "Experimental reversal of capillary blood flow," *Circulation*, vol. 4, no. 1, pp. 116–119, 1951.

[22] G. S. Kassab, J. A. Navia, K. March, and J. S. Choy, "Coronary venous retroperfusion: an old concept, a new approach," *Journal of Applied Physiology*, vol. 104, no. 5, pp. 1266–1272, 2008.

[23] B. M. Bernheim, "Arteriovenous anastomosisreversal of the circulationas a preventive of gangrene of the extremities: Review of the literature and report of six additional cases," *Annals of surgery*, vol. 55, no. 2, p. 195, 1912.

[24] D. F. Gerard, S. Gausewitz, R. Dilley, and E. Bernstein, "Acute physiologic effects of arteriovenous anastomosis and fistula in revascularizing the ischemic canine hind limb." *Surgery*, vol. 89, no. 4, pp. 485–493, 1981.

[25] K. Johansen and E. F. Bernstein, "Revascularization of the ischemic canine hindlimb by arteriovenous reversal," *Annals of surgery*, vol. 190, no. 2, pp. 243–253, 1979.

[26] L. Leger, "Essais de revascularisation dun membre par anastomose arterio-veineuse termino-terminale," *PRESSE MEDICALE*, vol. 57, no. 81, pp. 1198–1200, 1949.

[27] A. G. May, J. A. DeWeese, and C. G. Rob, "Arterialized in situ saphenous vein," *Archives of Surgery*, vol. 91, no. 5, pp. 743–750, 1965.

[28] J. E. Lavigne, J. C. Kerr, and K. G. Swan, "Hemodynamic effects of multiple arteriovenous fistulae in the canine hindlimb," *Journal of Surgical Research*, vol. 20, no. 6, pp. 571–574, 1976.

[29] A. Graham, A. Sniderman, S. Jothy, J. Homan, and J. Symes, "Staged reversal of venous flow for revascularization of the severely ischemic limb," *Journal of Surgical Research*, vol. 35, no. 1, pp. 11–20, 1983.

[30] A. M. Graham, R. Baffour, T. Burdon, B. Devarennes, M. A. Ricci, A. Common, R. Lisbona, A. D. Sniderman, and J. F. Symes, "A demonstration of vascular proliferation in response to arteriovenous reversal in the ischemic canine hind limb," *Journal of Surgical Research*, vol. 47, no. 4, pp. 341–347, 1989.

[31] L. Pu, A. D. Sniderman, Z. Arekat, A. M. Graham, R. Brassard, and J. F. Symes, "Angiogenic growth factor and revascularization of the ischemic limb: evaluation in a rabbit model," *Journal of Surgical Research*, vol. 54, no. 6, pp. 575–583, 1993.

[32] F. Lengua, "Technique darterialisation du rseau veineux du pied." *Presse Med*, vol. 4, p. 1039, 1975.

[33] R. Taylor, A.-M. Belli, and S. Jacob, "Distal venous arterialisation for salvage of critically ischaemic inoperable limbs," *The Lancet*, vol. 354, no. 9194, pp. 1962–1965, 1999.

[34] C. Engelke, R. A. Morgan, J. W. Quarmby, R. S. Taylor, and A.-M. Belli, "Distal venous arterialization for lower limb salvage: Angiographic appearances and interventional procedures 1," *Radiographics*, vol. 21, no. 5, pp. 1239–1248, 2001.

[35] V. L. Rowe, D. B. Hood, J. Lipham, T. Terramani, G. Torres, S. Katz, R. Kohl, and F. A. Weaver, "Initial experience with dorsal venous arch arterialization for limb salvage," *Annals of vascular surgery*, vol. 16, no. 2, pp. 187–192, 2002.

[36] P. Djoric, "Early individual experience with distal venous arterialization as a lower limb salvage procedure." *The American surgeon*, vol. 77, no. 6, pp. 726–730, 2011.

[37] F. Lengua, R. Cohen, B. L'Huillier, and J. Buffet, "Arteriovenous revascularization for lower limb salvage in unreconstructible arterial occlusive disease (long-term outcome)." *VASA. Zeitschrift fur Gefasskrankheiten*, vol. 24, no. 3, pp. 261–269, 1994.

[38] C. Özbek, M. Kestelli, B. Emrecan, İ. Özsöyler, K. Bayatli, H. Yaşa, B. Lafci, and A. Gürbüz, "A novel approach: ascending venous arterialization for atherosclerosis obliterans," *European journal of vascular and endovascular surgery*, vol. 29, no. 1, pp. 47–51, 2005.

[39] T. A. King, J. Marks, B. A. Berrettoni, and W. H. Seitz, "Arteriovenous reversal for limb salvage in unreconstructible upper extremity arterial occlusive disease," *Journal of vascular surgery*, vol. 17, no. 5, pp. 924–933, 1993.

[40] W. Xiao, J. Jiang, F. Tian, X. Li, and L. Tian, "Venous arterialization for the treatment of large-area foot skin retrograde avulsion," *Orthopedics*, vol. 36, no. 8, pp. e1091–e1095, 2013.

[41] "Fmrc: Manuals," http://fmrc.pulmcc.washington.edu/documents.shtml, [Accessed October 30, 2014].

[42] "Fluospheres fluorescent microspheres for blood flow determination," http://www.mobitec.com/probes/docs/media/pis/mp08829.pdf, 2002, [Accessed October 30, 2014].

[43] K. D. Budras, *Anatomy of the Dog*. Manson Publishing, 2007.

[44] H. Whiteman, "Peripheral artery disease: dramatically higher rates worldwide," http://www.medicalnewstoday.com/articles/264173.php, 2013, [Accessed October 30, 2014].

[45] "Amputee statistics you ought to know," http://www.advancedamputees.com/amputee-statistics-you-ought-know, 2012, [Accessed October 30, 2014].

[46] "Limb loss statistics," http://www.amputee-coalition.org/limb-loss-resource-center/resources-by-topic/limb-loss-statistics/limb-loss-statistics/index.html, 2014, [Accessed October 30, 2014].

[47] A. J. Feiring, M. Krahn, L. Nelson, A. Wesolowski, D. Eastwood, and A. Szabo, "Preventing leg amputations in critical limb ischemia with below-the-knee drug-eluting stents: the paradise (preventing amputations using drug eluting stents) trial," *Journal of the American College of Cardiology*, vol. 55, no. 15, pp. 1580–1589, 2010.

[48] R. J. Korthuis, D. N. Granger, and A. E. Taylor, "A new method for estimating skeletal muscle capillary pressure," *Am J Physiol*, vol. 246, no. 6 Pt 2, pp. H880–885, 1984.

[49] R. Braakman, P. Sipkema, and N. Westerhof, "Steady state and instantaneous pressure-flow relationships: characterisation of the canine abdominal periphery," *Cardiovascular research*, vol. 17, no. 10, pp. 577–588, 1983.

[50] N. Westerhof, R. Braakman, and P. Sipkema, "Small vessel compliance may explain peripheral pressure-flow relations," in *Vascular Dynamics*. Springer, 1989, pp. 95–107.

[51] S. Magder, "Starling resistor versus compliance. which explains the zero-flow pressure of a dynamic arterial pressure-flow relation?" *Circulation research*, vol. 67, no. 1, pp. 209–220, 1990.

[52] J. J. Maas, R. B. de Wilde, L. P. Aarts, M. R. Pinsky, and J. R. Jansen, "Determination of vascular waterfall phenomenon by bedside measurement of mean systemic filling pressure and critical closing pressure in the intensive care unit," *Anesthesia and analgesia*, vol. 114, no. 4, p. 803, 2012.

[53] P. Reymond, F. Merenda, F. Perren, D. Rüfenacht, and N. Stergiopulos, "Validation of a one-dimensional model of the systemic arterial tree," *American Journal of Physiology-Heart and Circulatory Physiology*, vol. 297, no. 1, pp. H208–H222, 2009.

[54] J. D. Coffman and J. A. Lempert, "Venous flow velocity, venous volume and arterial blood flow." *Circulation*, vol. 52, no. 1, pp. 141–145, 1975.

[55] P. Lewis, J. Psaila, R. Morgan, W. Davies, and J. Woodcock, "Common femoral artery volume flow in peripheral vascular disease," *British Journal of Surgery*, vol. 77, no. 2, pp. 183–187, 1990.

[56] R. Morgan, J. Psaila, J. Stone, G. Carolan, and J. Woodcock, "Postural changes in femoral artery blood flow in normal subjects, patients with peripheral vascular occlusive disease and patients undergoing lumbar sympathectomy, measured by duplex ultrasound flowmetry," *European journal of vascular surgery*, vol. 6, no. 4, pp. 408–415, 1992.

[57] G. L. Hammond, A. L. Davies, and W. G. Austen, "Retrograde coronary sinus perfusion: a method of myocardial protection in the dog during left coronary artery occlusion." *Annals of surgery*, vol. 166, no. 1, p. 39, 1967.

[58] J. S. Choy and G. S. Kassab, "A novel strategy for increasing wall thickness of coronary venules prior to retroperfusion," *American Journal of Physiology-Heart and Circulatory Physiology*, vol. 291, no. 2, pp. H972–H978, 2006.

[59] W. Ehrlich, R. Baer, R. Bellamy, and R. Randazzo, "Instantaneous femoral artery pressure-flow relations in supine anesthetized dogs and the effect of unilateral elevation of femoral venous pressure." *Circulation research*, vol. 47, no. 1, pp. 88–98, 1980.

[60] M. F. ORourke, "Pressure and flow waves in systemic arteries and the anatomical design of the arterial system," *J Appl Physiol*, vol. 23, no. 2, pp. 139–49, 1967.

[61] R. Braakman, P. Sipkema, and N. Westerhof, "Two zero-flow pressure intercepts exist in autoregulating isolated skeletal muscle," *Am J Physiol Heart Circ Physiol*, vol. 258, pp. H1806–H1814, 1990.

[62] D. Kopelman, G. Hirshhorn, and M. Hashmonai, "Prevention of limb loss in critical ischaemia by arterialization of the superficial venous system: an experimental study in dogs," *Vascular*, vol. 6, no. 4, pp. 384–388, 1998.

[63] S. M. Gifford, B. W. Propper, and J. L. Eliason, "The ischemic threshold of the extremity," *Perspectives in vascular surgery and endovascular therapy*, vol. 23, no. 2, pp. 81–87, 2011.

[64] I. Forrest, T. Lindsay, A. Romaschin, and P. Walker, "The rate and distribution of muscle blood flow after prolonged ischemia," *Journal of vascular surgery*, vol. 10, no. 1, pp. 83–88, 1989.

[65] F. W. Blaisdell, "The pathophysiology of skeletal muscle ischemia and the reperfusion syndrome: a review," *Vascular*, vol. 10, no. 6, pp. 620–630, 2002.

[66] O. Raza and R. Schlichtig, "during dysoxia 2 metabolic component of intestinal pco," *J Appl Physiol*, vol. 89, pp. 2422–2429, 2000.

[67] T. S. Westvik, T. N. Fitzgerald, A. Muto, S. P. Maloney, J. M. Pimiento, T. T. Fancher, D. Magri, H. H. Westvik, T. Nishibe, O. C. Velazquez *et al.*, "Limb ischemia after iliac ligation in aged mice stimulates angiogenesis without arteriogenesis," *Journal of vascular surgery*, vol. 49, no. 2, pp. 464–473, 2009.

[68] R. E. Waters, R. L. Terjung, K. G. Peters, and B. H. Annex, "Preclinical models of human peripheral arterial occlusive disease: implications for investigation of therapeutic agents," *Journal of Applied Physiology*, vol. 97, no. 2, pp. 773–780, 2004.

[69] A. Hellingman, A. Bastiaansen, M. de Vries, L. Seghers, M. Lijkwan, C. Löwik, J. Hamming, and P. Quax, "Variations in surgical procedures for hind limb ischaemia mouse models result in differences in collateral formation," *European Journal of Vascular and Endovascular Surgery*, vol. 40, no. 6, pp. 796–803, 2010.

[70] S. L. Rosenthal and A. C. Guyton, "Hemodynamics of collateral vasodilatation following femoral artery occlusion in anesthetized dogs," *Circulation research*, vol. 23, no. 2, pp. 239–248, 1968.

[71] L. S. Brevetti, R. Paek, S. E. Brady, J. I. Hoffman, R. Sarkar, and L. M. Messina, "Exercise-induced hyperemia unmasks regional blood flow deficit in experimental hindlimb ischemia," *Journal of Surgical Research*, vol. 98, no. 1, pp. 21–26, 2001.

[72] M. A. Ziegler, M. R. DiStasi, R. G. Bills, S. J. Miller, M. Alloosh, M. P. Murphy, A. George Akingba, M. Sturek, M. C. Dalsing, and J. L. Unthank, "Marvels, mysteries, and misconceptions of vascular compensation to peripheral artery occlusion," *Microcirculation*, vol. 17, no. 1, pp. 3–20, 2010.

[73] M. Conrad, J. Anderson 3rd, and J. Garrett Jr, "Chronic collateral growth after femoral artery occlusion in the dog." *Journal of applied physiology*, vol. 31, no. 4, pp. 550–555, 1971.

[74] G. Kvarstein, P. Mirtaheri, and T. I. Tønnessen, "Detection of ischemia by pco2 before adenosine triphosphate declines in skeletal muscle," *Critical care medicine*, vol. 32, no. 1, pp. 232–237, 2004.

[75] C. Ozek, F. Zhang, W. Lineaweaver, B. Chin, L. Newlin, T. Eiman, and H. Buncke, "Arterialization of the venous system in a rat lower limb model," *British journal of plastic surgery*, vol. 50, no. 6, pp. 402–407, 1997.

[76] N. M. Matolo, S. E. Cohen, and E. F. Wolfman Jr, "Use of an arteriovenous fistula for treatment of the severely ischemic extremity: experimental evaluation." *Annals of surgery*, vol. 184, no. 5, p. 622, 1976.

[77] S. Whittaker and F. Winton, "The apparent viscosity of blood flowing in the isolated hindlimb of the dog, and its variation with corpuscular concentration," *The Journal of physiology*, vol. 78, no. 4, pp. 339–369, 1933.

[78] G. A. Van Huis, P. Sipkema, and N. Westerhof, "Instantaneous and steady-state pressure-flow relations of the coronary system in the canine beating heart," *Cardiovascular research*, vol. 19, no. 3, pp. 121–131, 1985.

[79] H. Dardik, "The distal arteriovenous fistula: A useful adjunct or a passing fancy?" *European journal of vascular surgery*, vol. 2, no. 2, pp. 67–69, 1988.

[80] J. G. Younger, J. L. Falk, and S. G. Rothrock, "Relationship between arterial and peripheral venous lactate levels," *Academic Emergency Medicine*, vol. 3, no. 7, pp. 730–733, 1996.

[81] L. Pu, S. Jackson, K. J. Lachapelle, Z. Arekat, A. M. Graham, R. Lisbona, R. Brassard, S. Carpenter, and J. F. Symes, "A persistent hindlimb ischemia model in the rabbit," *Investigative Surgery*, vol. 7, no. 1, pp. 49–60, 1994.

[82] A. Kabaroudis, T. Gerassimidis, D. Karamanos, B. Papaziogas, V. Antonopoulos, and A. Sakantamis, "Metabolic alterations of skeletal muscle tissue after prolonged acute ischemia and reperfusion," *Investigative Surgery*, vol. 16, no. 4, pp. 219–228, 2003.

[83] W. Kuzon Jr, P. Walker, D. Mickle, K. Harris, B. Pynn, and N. McKee, "An isolated skeletal muscle model suitable for acute ischemia studies," *Journal of Surgical Research*, vol. 41, no. 1, pp. 24–32, 1986.

[84] R. J. Connett, T. E. Gayeski, and C. R. Honig, "Lactate accumulation in fully aerobic, working, dog gracilis muscle," *Am J Physiol*, vol. 246, no. 1 Pt 2, pp. H120–H128, 1984.

[85] C. H. Dart Jr, G. Johnson Jr, R. M. Peters, and N. A. Womack, "Hemodynamic effects of femoral venous occlusion before and after an acute arteriovenous fistula." *Annals of surgery*, vol. 164, no. 2, p. 190, 1966.

[86] R. W. Hobson II and C. B. Wright, "Peripheral side to side arteriovenous fistula: Hemodynamics and application in venous reconstruction," *The American Journal of Surgery*, vol. 126, no. 3, pp. 411–414, 1973.

[87] R. E. Scully and C. W. Hughes, "The pathology of ischemia of skeletal muscle in man: A description of early changes in muscles of the extremities following damage to major peripheral arteries on the battlefield," *The American journal of pathology*, vol. 32, no. 4, p. 805, 1956.

[88] V. van Weel, D. Eefting, P. Quax, P. Madeddu, C. Emanueli, F. Spillmann, M. Meloni, N. Bouby, C. Richer, F. Alhenc-Gelas *et al.*, "Murine models of limb ischemia," *Growing Blood Vessels to Treat Limb Ischemia*, vol. 45, no. 5, p. 47, 2007.

[89] P. M. Levin, N. M. Rich, J. E. Hutton, W. F. Barker, and J. A. Zeller, "Role of arteriovenous shunts in venous reconstruction," *The American Journal of Surgery*, vol. 122, no. 2, pp. 183–191, 1971.